

## What Is an Effective Way to Measure Arterial Demand When It Exceeds Capacity?

[http://www.virginiadot.org/vtrc/main/online\\_reports/pdf/22-r19.pdf](http://www.virginiadot.org/vtrc/main/online_reports/pdf/22-r19.pdf)

**MECIT CETIN, Ph.D.**  
Professor  
Department of Civil Engineering

**HONG YANG, Ph.D.**  
Associate Professor  
Department of Computational Modeling, Simulation and Engineering

**KUN XIE, Ph.D.**  
Assistant Professor  
Department of Civil Engineering

**GIRIDHAR KATTEPOGU**  
Graduate Research Assistant  
Department of Civil Engineering

**BEHROUZ SALAHSHOUR**  
Graduate Research Assistant  
Department of Civil Engineering

Old Dominion University

Final Report VTRC 22-R19

**Standard Title Page - Report on Federally Funded Project**

1. Report No.: FHWA/VTRC 22-R19	2. Government Accession No.:	3. Recipient's Catalog No.:	
4. Title and Subtitle: What Is an Effective Way to Measure Arterial Demand When It Exceeds Capacity?		5. Report Date: December 2021	
		6. Performing Organization Code:	
7. Author(s): Mecit Cetin, Ph.D., Hong Yang, Ph.D., Kun Xie, Ph.D., Giridhar Kattepogu, and Behrouz Salahshour		8. Performing Organization Report No.: VTRC 22-R19	
9. Performing Organization and Address: Virginia Transportation Research Council 530 Edgemont Road Charlottesville, VA 22903		10. Work Unit No. (TRAIS):	
		11. Contract or Grant No.: 116572	
12. Sponsoring Agencies' Name and Address: Virginia Department of Transportation      Federal Highway Administration 1401 E. Broad Street                              400 North 8th Street, Room 750 Richmond, VA 23219                                Richmond, VA 23219-4825		13. Type of Report and Period Covered: Final Contract	
		14. Sponsoring Agency Code:	
15. Supplementary Notes: This is an SPR-B report.			
16. Abstract: This project focused on developing and evaluating methods for estimating demand volume for oversaturated corridors. Measuring demand directly with vehicle sensors is not possible when demand is larger than capacity for an extended period, as the queue grows beyond the sensor, and the flow measurements at a given point cannot exceed the capacity of the section. The main objective of the study was to identify and develop methods that could be implemented in practice based on readily available data. To this end, two methods were proposed: an innovative method based on shockwave theory; and the volume delay function adapted from the Highway Capacity Manual. Both methods primarily rely on probe vehicle speeds (e.g., from INRIX) as the input data and the capacity of the segment or bottleneck being analyzed. The proposed methods were tested with simulation data and validated based on volume data from the field. The results show both methods are effective for estimating the demand volume and produce less than 4% error when tested with field data.			
17 Key Words:		18. Distribution Statement: No restrictions. This document is available to the public through NTIS, Springfield, VA 22161.	
19. Security Classif. (of this report): Unclassified	20. Security Classif. (of this page): Unclassified	21. No. of Pages: 56	22. Price:

**FINAL REPORT**

**WHAT IS AN EFFECTIVE WAY TO MEASURE ARTERIAL DEMAND WHEN IT  
EXCEEDS CAPACITY?**

**Mecit Cetin, Ph.D.**  
**Professor**  
**Department of Civil Engineering**  
**Old Dominion University**

**Hong Yang, Ph.D.**  
**Associate Professor**  
**Department of Computational Modeling, Simulation and Engineering**  
**Old Dominion University**

**Kun Xie, Ph.D.**  
**Assistant Professor**  
**Department of Civil Engineering**  
**Old Dominion University**

**Giridhar Kattapogu**  
**Graduate Research Assistant**  
**Department of Civil Engineering**  
**Old Dominion University**

**Behrouz Salahshour**  
**Graduate Research Assistant**  
**Department of Civil Engineering**  
**Old Dominion University**

*VTRC Project Manager*  
John Miller, Ph.D., P.E., Virginia Transportation Research Council

In Cooperation with the U.S. Department of Transportation  
Federal Highway Administration

Virginia Transportation Research Council  
(A partnership of the Virginia Department of Transportation  
and the University of Virginia since 1948)

Charlottesville, Virginia

December 2021  
VTRC 22-R19

## **DISCLAIMER**

The project that is the subject of this report was done under contract for the Virginia Department of Transportation, Virginia Transportation Research Council. The contents of this report reflect the views of the author(s), who is responsible for the facts and the accuracy of the data presented herein. The contents do not necessarily reflect the official views or policies of the Virginia Department of Transportation, the Commonwealth Transportation Board, or the Federal Highway Administration. This report does not constitute a standard, specification, or regulation. Any inclusion of manufacturer names, trade names, or trademarks is for identification purposes only and is not to be considered an endorsement.

Each contract report is peer reviewed and accepted for publication by staff of the Virginia Transportation Research Council with expertise in related technical areas. Final editing and proofreading of the report are performed by the contractor.

Copyright 2021 by the Commonwealth of Virginia.  
All rights reserved.

## **ABSTRACT**

This project focused on developing and evaluating methods for estimating demand volume for oversaturated corridors. Measuring demand directly with vehicle sensors is not possible when demand is larger than capacity for an extended period, as the queue grows beyond the sensor, and the flow measurements at a given point cannot exceed the capacity of the section. The main objective of the study was to identify and develop methods that could be implemented in practice based on readily available data. To this end, two methods were proposed: an innovative method based on shockwave theory; and the volume delay function adapted from the Highway Capacity Manual. Both methods primarily rely on probe vehicle speeds (e.g., from INRIX) as the input data and the capacity of the segment or bottleneck being analyzed. The proposed methods were tested with simulation data and validated based on volume data from the field. The results show that both methods are effective for estimating the demand volume and produce less than 4% error when tested with field data.



## TABLE OF CONTENTS

INTRODUCTION .....	1
PURPOSE AND SCOPE.....	2
METHODS .....	3
Overview.....	3
Literature Review.....	3
Methods for Demand Volume Estimation .....	3
Simulation and Field Data for Model Testing and Validation.....	7
RESULTS .....	13
Literature Review.....	13
Application of the Demand Estimation Methods Using Simulation Data .....	18
Validation of the Methods on the Field Data.....	25
DISCUSSION.....	29
CONCLUSIONS.....	30
RECOMMENDATIONS .....	30
IMPLEMENTATION AND BENEFITS .....	31
Implementation .....	31
Benefits .....	33
ACKNOWLEDGMENTS .....	34
REFERENCES .....	34
APPENDIX A: Steps in Applying the SW and VDF methods.....	41
Step 1: Identifying an XD or TMC Segment Along the Oversaturated Corridor.....	41
Step 2: Extracting key parameters from the XD or TMC speed profiles.....	45
Step 3: Applying the SW and HCM VDF methods .....	46
APPENDIX B: Traffic Counts.....	49



## **FINAL REPORT**

### **WHAT IS AN EFFECTIVE WAY TO MEASURE ARTERIAL DEMAND WHEN IT EXCEEDS CAPACITY?**

**Mecit Cetin, Ph.D.**  
**Department of Civil Engineering**  
**Old Dominion University**

**Kun Xie, Ph.D.**  
**Department of Civil Engineering**  
**Old Dominion University**

**Hong Yang, Ph.D.**  
**Department of Computational Modeling, Simulation and Engineering**  
**Old Dominion University**

**Giridhar Kattepogu**  
**Graduate Research Assistant**  
**Department of Civil Engineering**  
**Old Dominion University**

**Behrouz Salahshour**  
**Graduate Research Assistant**  
**Department of Civil Engineering**  
**Old Dominion University**

## **INTRODUCTION**

Quantifying travel demand is an essential element in both transportation planning and operations since key performance measures (e.g., benefit-cost ratios, travel delays, emissions) depend heavily on the demand level. To select and prioritize transportation projects for investment, the Virginia Department of Transportation (VDOT) uses an outcome-based process called System Management and Allocation of Resources for Transportation: Safety, Congestion, Accessibility, Land Use, Economic Development and Environment (SMART SCALE) for project screening, scoring, and evaluation. SMART SCALE requires certain evaluation measures to quantify the benefits of each potential project. Some of the calculated measures include person throughput, person hours of delay, travel time reliability, crash rates, and air quality and environmental effects. To calculate or estimate these measures, VDOT employs established models and methods that require various types of input data. While demand is one of the key inputs to these methods, VDOT currently does not have a common approach for measuring demand when traffic volume exceeds the capacity of the roadway facilities. Hence, there is a strong need to identify the best practices and solutions for determining the demand volume (DV) to be used in the SMART SCALE project prioritization process and other VDOT applications.

This report uses “DV” to refer to demand volume or demand rate (e.g., measured in vehicles per hour) when it exceeds capacity.

In general, when demand is less than the capacity of a facility, the flow rate measured by traffic detectors (i.e., volume counters) at the subject facility will be identical to the demand. However, when demand is greater than the capacity, measuring or estimating DV becomes very challenging, resulting in oversaturated conditions and long queues spread over the network. Under such conditions, measuring demand with the commonly available sensors (e.g., loop detectors) in the field is generally not possible. While more advanced sensing technologies (e.g., cameras, aerial videos, vehicle tracking and identification) would help capture queuing and origin-destination movements, these technologies are costly and not commonly deployed for demand estimation.

To address this challenge, researchers have proposed several approaches such as incorporating observed queueing dynamics into demand prediction and capitalizing on and calibrating the volume-delay functions or speed-flow equations. More details about these studies are provided in the Literature Review section. This study proposes two potential methods for estimating DV for oversaturated conditions. Both methods rely primarily on commonly available speed data generated by probe vehicles or vehicle-tracking technologies, such as INRIX probe data.

The first method makes use of shockwave theory and involves determining the critical times when the queue reaches the end or beginning of a road segment. INRIX data are available for Traffic Message Channel (TMC) and eXtreme Definition (XD) segments. Both refer to defined road segments for reporting and aggregating traffic data, and XD segments are generally shorter than TMC segments. By analyzing the speed profiles of given TMC or XD segments, one can infer the evolution of queuing over the congested corridor. This report describes how INRIX data alone can be used to estimate a  $v/c$  ratio for the oversaturated segment. This innovative method allows estimating the DV when the capacity of the segment or bottleneck is known. The second method relies on the volume delay function (VDF) from the Highway Capacity Manual (HCM) for oversaturated conditions. The delay value for the VDF is extracted from INRIX speed data for a given TMC or XD segment. The VDF is then solved for the unknown demand for the defined conditions.

The rest of the report presents the scope of this project, literature review, the methodologies followed, data collection process, the application of the methods on simulation and field data, conclusions, recommendations, and implementation and benefits of the study.

## **PURPOSE AND SCOPE**

The overall goal of this proposed project was to identify an effective way to estimate arterial demand when its capacity is exceeded. Given a congested arterial, the demand volume refers to the arrival flow rate in the upstream of the bottleneck in the peak periods. The specific objectives are listed below.

- Survey and document applicable methods for measuring and estimating demand.

- Identify the strengths and weaknesses of these methods and discuss their suitability for potential VDOT applications.
- Evaluate and compare promising methods in case studies.
- Recommend how the most promising methods may be used by VDOT.

The focus of this project was to identify a method for demand estimation that can be implemented by VDOT in its SMART SCALE process or for other applications. Estimating origin-destination demand for travel demand models (TDMs) was beyond the scope of this project, and the emphasis is on arterials, not freeway facilities. The focus was on the major movements along arterials rather than the individual turning movements. To evaluate alternative methods, the research team used a hybrid approach that involves both microscopic simulation modeling and field data collection and processing.

While travel demand is a broad topic, the focus of this project was on estimating demand of a given facility under prevailing (oversaturated) conditions. This entailed incorporating the queuing dynamics observed in the field into the demand estimation. It is possible that demand for a given facility may change after improvements are made. However, characterizing such induced or latent demand requires a TDM that was outside the scope of this study.

## **METHODS**

### **Overview**

The following tasks were conducted to achieve the study objectives:

1. Literature review
2. Development of methods for demand volume estimation
3. Data collection for model testing

### **Literature Review**

The research team conducted a literature review that included a survey of existing methods for estimating volume and related traffic flow parameters based on various types of sensor data. Since estimating demand volume for oversaturated corridors is highly related to queue dynamics, methods for predicting queue lengths were also reviewed and summarized. Alternative approaches to estimate volume, e.g., through volume delay functions or travel time-volume relationships, are also discussed, as are the various types of intelligent transportation systems data used in predicting travel demand and traffic flow parameters. Methods making use of data from vehicle detectors, probe vehicles and Connected Vehicles (CV), and video surveillance were also reviewed and synthesized.

### **Methods for Demand Volume Estimation**

As discussed in greater depth in the literature review section, various approaches are used to estimate demand volume by employing different types of sensor data (e.g., aerial/drone imagery, probe vehicle trajectory). However, for oversaturated corridors, there is no well-

established method that can be implemented in practice with a reasonable level of effort based on readily available data. VDOT has access to INRIX probe data through the Reginald Integrated Transportation Information System (RITIS, 2021) and such data are readily available for both freeways and arterials. Furthermore, over the years, the granularity of the INRIX data and the sample size or trips being captured by INRIX are increasing. Therefore, the research team proposed two methods that primarily rely on INRIX speed data for estimating the demand volume. These two approaches are listed below and presented in more details in the following subsections.

- *Shockwave Theory Based Approach*: When the demand exceeds capacity, the queue grows upstream of the intersection at a rate (or speed) proportional to the demand volume and the throughput (or capacity) of the intersection. The boundary between congested (high density) traffic and arriving (low density) traffic is called a shockwave and can be observed in the field as the back of the queue grows at a steady rate. In the proposed model, the shockwave speed is estimated from the INRIX data which is then utilized to estimate the demand volume. For brevity, this first method is referred to as the SW method in this report.
- *Highway Capacity Manual (HCM) 's Volume Delay Function (VDF)*: The HCM provides a formula for calculating the average delay per vehicle when the signalized intersection is oversaturated. Average delay is calculated for a given volume to capacity ratio (denoted as 'X' or  $v/c$ ). For our application, the delay is known (from INRIX data), and the HCM equation is solved for the unknown  $v/c$  ratio so that the demand volume can be estimated. For brevity, this method is referred to as the VDF method in this report.

Before these two methods are presented, it is important to analyze how a typical INRIX speed profile looks like for an oversaturated corridor. Figure 1 shows the speed profiles for three days for a TMC segment on US-28 SB in Northern Virginia, a heavily congested corridor. It is apparent that at around 2 PM speeds are consistently dropping from 55 mph (denoted as  $U_A$ ) to approximately 20 mph and staying at the low level ( $U_C$ ) for a while before going back higher.

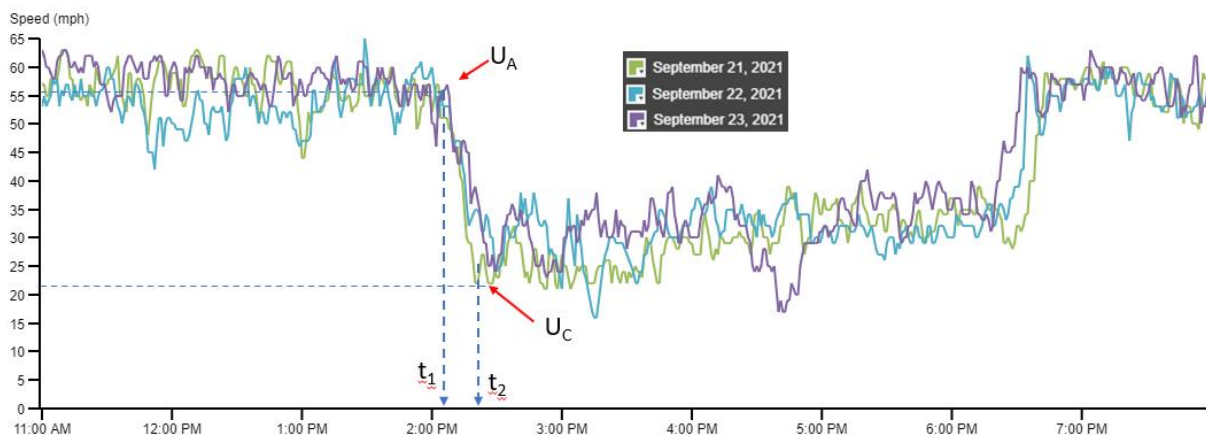


**Figure 1. INRIX speed profiles for TMC 110-05669 on US-28 (Sully Rd) southbound. This TMC is 1.18 mi long and ends at the Walney Rd/Braddock Rd Intersection.**

This type of pattern (i.e., speeds dropping and staying constant for a while before resuming back to free-flow speeds) has been observed at various other congested segments. This pattern can be explained by the fact that the TMC length is finite (1.18mi for this TMC) and speed values are computed based on the probe vehicles travelling within the TMC boundaries. As the queue grows upstream, it eventually reaches the beginning of the TMC segment. As long as the queue (or congestion) spans the entire length of the TMC segment, and the downstream conditions remain stable, the probe vehicle speeds will remain approximately constant (since the boundary conditions remain the same).

For such oversaturated segments, this pattern provides useful information in understanding the queue dynamics and the propagation of congestion. For example, one can estimate the time when the queue reaches the beginning of the TMC segment, which would be  $t_2$  for the sample data in Figure 1. Since, the length of the segment is known, the speed by which the queue grows (i.e., shockwave speed) can be computed by simply dividing the segment length by  $t_2-t_1$ . This fundamental observation is the basis for the new shockwave-based method described below for DV estimation.

### Shockwave Theory-Based Method

Traffic conditions on a roadway can be described in terms of speed, density, or flow at a macroscopic level. Due to the variations and fluctuations in demand and capacity, the traffic conditions (or system state) change over time and space. When two different traffic flow states interact, a boundary is established that demarcates the time-space domain of one flow state from the other. This boundary is called a shockwave. A prominent example of this could be observed at an oversaturated corridor as high-speed vehicles approach a queue of stopped vehicles. The boundary that separates the congestion from arriving traffic can be observed to move upstream as the queue grows. The rate at which this queue grows or, equivalently, the speed at which the shockwave travels ( $w$ ), is correlated to the flow rate of the arriving traffic ( $q_A$ ), the flow rate within the queue ( $q_C$ ), and the densities of the arriving ( $k_A$ ) and queued ( $k_C$ ) traffic. From the basics of traffic flow theory, this relationship is described as:

$$w = \frac{q_A - q_C}{k_A - k_C} \quad (1)$$

This basic relationship is employed to estimate the arriving flow rate ( $q_A$ ) or the demand volume for oversaturated conditions. Since measuring density is generally more difficult than the other two traffic flow variables, density can be replaced by its equivalent using the fundamental relationship among the three-traffic flow variables, i.e., density is flow divided by speed ( $k = q/u$ ). Therefore, Equation (1) can be rearranged as follows for the unknown arrival rate  $q_A$ .

$$q_A = \frac{q_C - w \frac{q_C}{u_C}}{1 - \frac{w}{u_A}} \quad (2)$$

To apply the model above, the quantities on the right-hand side need to be provided. It should be noted that traffic conditions are dynamic, therefore these quantities would be time dependent. Therefore, the analysis will pertain to a specific period. As explained earlier, by analyzing the INRIX speed profiles (see Figure 1), one can estimate the critical time at which the queue reaches the beginning of the TMC or XD segment. In Figure 1, this corresponds to  $t_2$ , while  $t_1$  can be considered the beginning of the oversaturation period. If these two event times are captured reliably, then one can estimate how long it takes for the queue to reach the beginning of the segment by simply subtracting  $t_1$  from  $t_2$ . If this is denoted by  $T$  (i.e.,  $T = t_2 - t_1$ ), the average shockwave speed will simply be  $L/T$ , where  $L$  is the segment length. To use equation (2) in demand volume estimation, the other required inputs are as follows:

- *The flow rate within the queue,  $q_c$* : This will approximately be equal to the discharge or throughput from the signalized intersection that is acting as the bottleneck. At a typical signalized intersections approach, this can be estimated by dividing the total turning volumes (left, right, and through) by the observation period. If counts are not available, the capacity of the approach can be approximated by the HCM methods for signalized intersections.
- *The speed of the arriving traffic,  $u_A$* : This can be taken as the speed before the oversaturation starts. In Figure 1, this speed value is approximately 55 mph.
- *The speed of the queued traffic,  $u_c$* : This can be taken as the stable speed after the queue reaches the beginning of the segment. In Figure 1, this speed value is approximately 22 mph.

Equation (2) can be rearranged to solve for the  $v/c$  ratio instead of the demand volume. Dividing both sides by flow rate  $q_c$ , i.e., the queue discharge flow, results in the following.

$$q_A/q_c = \frac{1 - w/u_c}{1 - w/u_A} \quad (3)$$

The expression above can be used to estimate a  $v/c$  ratio for the oversaturated segment. It is apparent that the only input needed are three speeds:  $w$ ,  $u_A$ , and  $u_c$ . All three values can be extracted from the INRIX speed data.

### **HCM Volume Delay Function**

To evaluate the level of service for signalized intersection, the HCM presents an analytical method to estimate the control delay (TRB, 2000). Equation (4) shows how the incremental delay caused by oversaturation is estimated using the HCM method. This Volume Delay Function (VDF) takes the degree of saturation  $X$  (or volume to capacity ratio), capacity of the lane group  $c$  (or intersection approach), and two parameters related to the signal operations ( $k$  and  $I$ ) as inputs to compute the average delay for the analysis period of interest  $T$ . The equation assumes that there is no residual queue at the start of the analysis period. This equation is applicable to all degrees of saturations.

$$d_2 = 900 T \left[ (X - 1) + \sqrt{(X - 1)^2 + \frac{8kIX}{cT}} \right] \quad (4)$$

Where:

- $d_2$  = incremental delay to account for effect of random and oversaturation queues, adjusted for duration of analysis period and type of signal control (s/veh);
- $T$  = duration of analysis period (h);
- $k$  = incremental delay factor that is dependent on controller settings;
- $I$  = upstream filtering/metering adjustment factor;
- $c$  = lane group capacity (vehicles/hour); and
- $X$  = lane group v/c ratio or degree of saturation.

For the purpose of this project, Equation (5) needs to be solved for the degree of saturation  $X$  (i.e., volume to capacity ratio) for the measured average delay  $d_2$ . The delay value will be extracted from INRIX speed data for a given TMC or XD segment with a known length,  $L$ . Since  $d_2$  is the average delay per vehicle, it is computed as:

$$d_2 = \frac{\frac{L}{u_C} - \frac{L}{u_A}}{2} \quad (5)$$

The remaining terms in Equation (4) include  $T$ ,  $k$ ,  $I$ , and  $c$ .  $T$  is the analysis period and taken to be  $t_2 - t_1$ . The values for the parameters  $k$  and  $I$  can be found from the HCM tables (Exhibit 16-13 for  $k$  values and Exhibit 15-9 for  $I$  in HCM 2000 (TRB, 2000)). The capacity  $c$  is the intersection approach throughput and is the same as parameter  $q_C$  as defined above. With these inputs, the best  $X$  value satisfying Equation (4) is found by minimizing the square of the difference between the observed delay from INRIX data (Equation 5) and the incremental delay ( $d_2$ ) from equation (4). The Solver function in MS Excel can be utilized for this purpose.

### **Simulation and Field Data for Model Testing and Validation**

To evaluate the methods described above, the research team utilized both simulation and field data. For generating the simulated data, two networks were simulated in VISSIM: A 2.6 km stretch of a two-lane road with a traffic signal; and a section of Indian River Road, a major arterial in Virginia Beach. For both simulation models, the traffic demands loaded onto the network are hypothetical and larger than the intersection capacity. Volume data from a congested corridor were collected to validate the models. These are explained below.

#### **Simulation Data: Two-Lane Road**

Hypothetical demand scenarios were created in VISSIM, a microscopic simulation program, to generate travel speeds and other needed data. First, a 2.6 km two-lane road segment with a signalized intersection is created in VISSIM to generate data for a basic scenario where only through movements are modeled. A fixed-time traffic signal is placed at 2.5 km from the

beginning of the segment, with a 45 second red phase and a 45 second green phase. Demand is loaded onto the network by specifying the flow rates shown in Figure 2. All other VISSIM input parameters were kept at default values to generate data for this hypothetical network. The maximum input flow rate of 2,400 vehicles/hour is larger than the capacity of the signalized intersection (which is about 1,950 vehicles/hour) and causes the queue to grow rapidly as shown in Figure 3. The analyses shown in the next section were performed solely based on the trajectory data extracted from VISSIM which include position and speed for every vehicle at every simulation second. The statistical programming language R was used to process the data and apply the methods. To emulate TMC-like data, the trajectory data were partitioned into discrete spatiotemporal regions. Since INRIX data’s lowest time resolution is one minute, the time resolution was set to one minute. Since TMC or XD segment lengths can vary, a range of TMC lengths, from 250 meters to 2000 meters in increments of 250 meters (for a total of 8 length scenarios), were considered. Each one of these TMCs starts at the upstream of the signal and terminates at the stop bar. To generate the speed data for each TMC, average speeds of all vehicles within the TMC boundaries were calculated. The two methods described above were then applied to the average speed data for each TMC scenario.

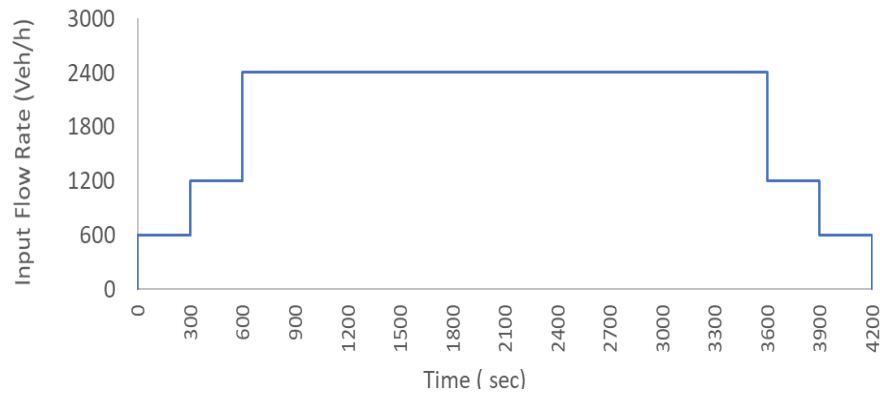


**Figure 2. Demand profile loaded onto the VISSIM network**

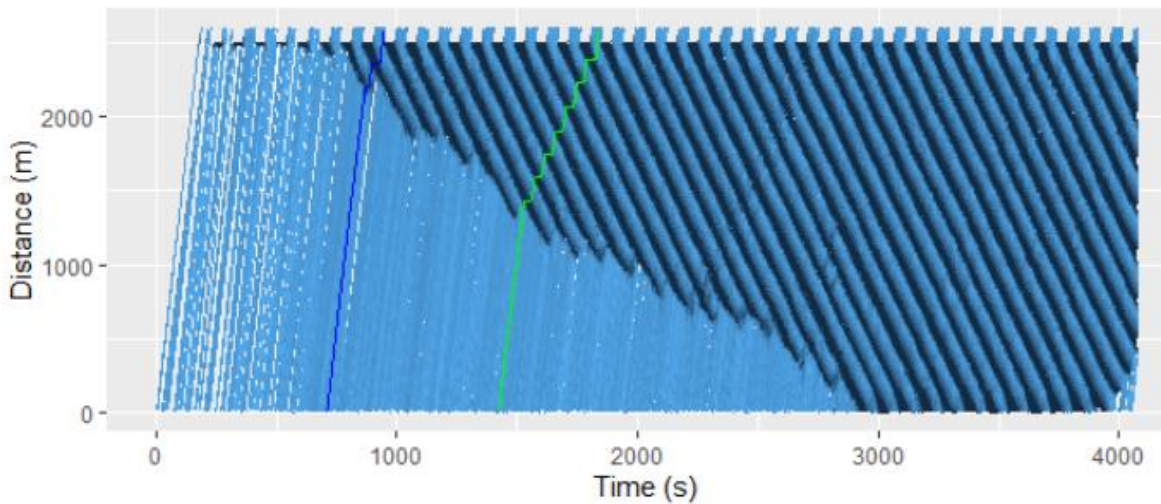


**Figure 3. Vehicle trajectories for the simulated oversaturated condition. Two sample trajectories are highlighted (blue and green) for a better visualization.**

## Simulation Data: Indian River Road Corridor

To generate data for a more complex setting, the team created a VISSIM network for the eastbound direction of the Indian River Road (IRR) corridor shown in Figure 4. Two signalized intersections were modeled: one at the intersection of Regent University Drive and the other at Centerville Turnpike. Traffic signal times for these two intersections were coded in VISSIM based on the timing plans received from the City of Virginia Beach for the PM peak. Turning volume percentages at the intersections were based on field counts. Four hypothetical demand scenarios were considered for the vehicles entering the network at the beginning of the IRR corridor. Vehicles also enter the network at the two ramps shown in Figure 5. These demand profiles are shown in Figure 6. The ramp volumes were kept at a constant rate of 100 vehicles/hour in all scenarios except in scenario 4, where the entering flow for Ramp-2 was set to 1,000 vehicles/hour.

These arbitrary demands are large enough to create oversaturation in the corridor. Each scenario was run four times with different random seeds. The trajectory data were generated from VISSIM and processed for creating XD speed profiles needed for the demand estimation methods. The trajectories were segmented spatially based on the INRIX XD definitions for the corridor shown in Figure 5. For each XD segment, average speeds were calculated at one minute aggregation intervals from the trajectory data of all vehicles. These speed profiles were then utilized in the demand estimation methods.

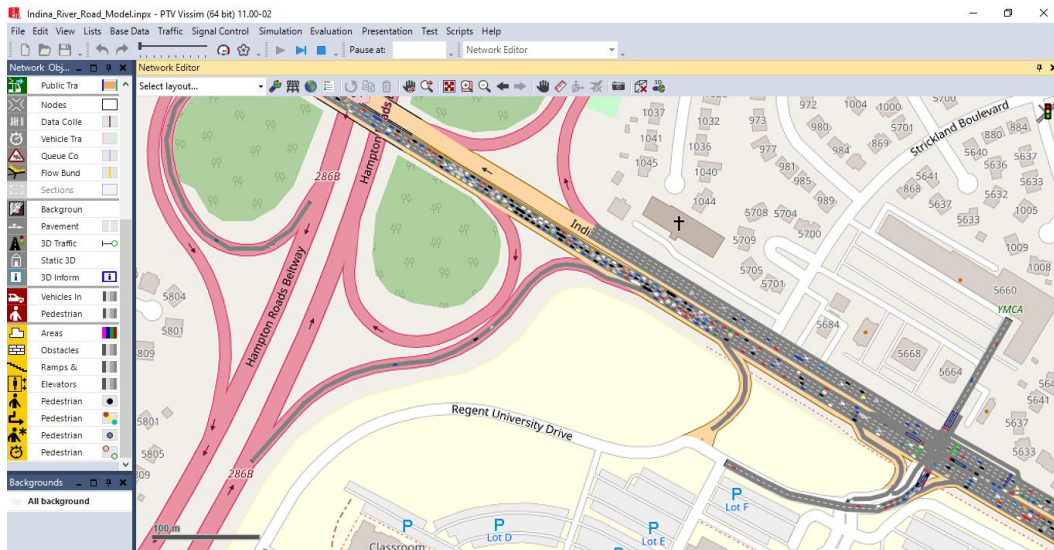


Figure 4. Screenshot of the VISSIM network for the IRR corridor

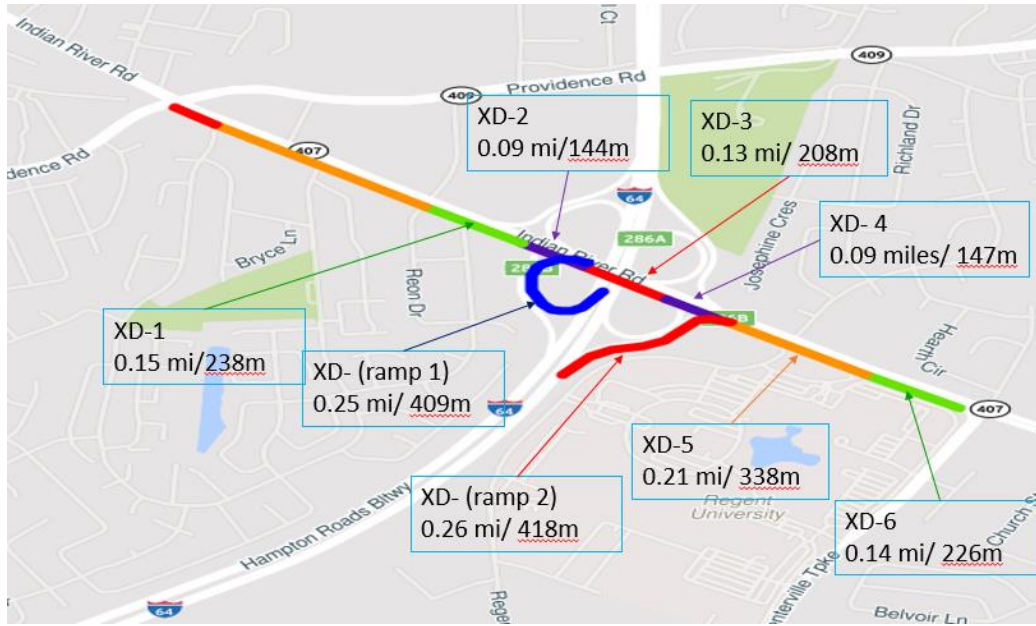


Figure 5. INRIX XD segments for the modeled portion of the IRR corridor

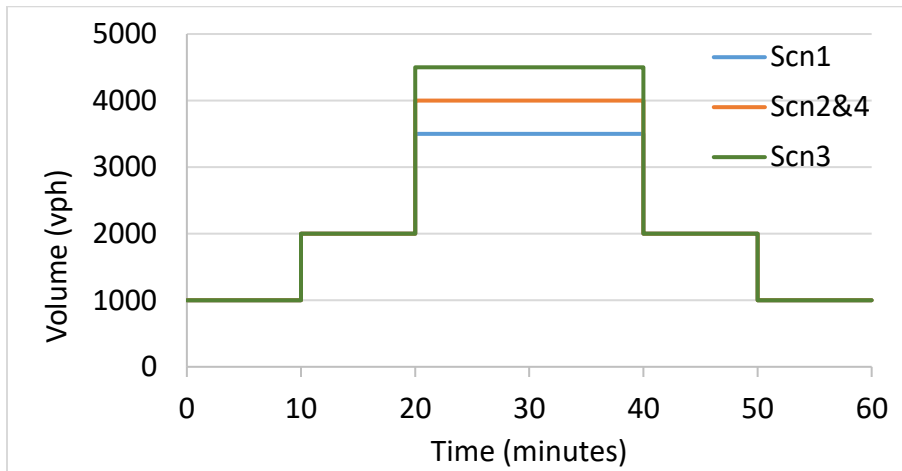


Figure 6. Demand profiles for the mainline volume entering the IRR corridor under the four scenarios

## Field Data Collection

To test the methods with field data, traffic volume counts are needed for oversaturated corridors. Since INRIX data have one-minute resolution, these counts need to be at one-minute or lower aggregation levels to be able to extract the needed flow rates within the period of interest (i.e., T). Ideally, the selected corridor should have vehicle detectors both upstream and downstream of the segment being studied. Furthermore, the (TMC or XD) segment being studied should be long enough for vehicles to accumulate for a meaningful duration before the queue spills back to the upstream segment. In the Results section, the impacts of the segment length on model accuracy are analyzed with the simulation data.

To validate the methods with field data, two data sources were explored. First, Automated Traffic Signal Performance Measures (ATSPM) data were processed for a group of intersections on US 29 in Northern Virginia. ATSPM include high-resolution data from traffic signal infrastructure and contain event times for each sensor activation (sensor on) and deactivation (sensor off) events. The team received the raw ATSPM data from VDOT for the US 29 corridor (intersections 1-8 in Figure 7) and prepared R scripts to convert the data to traffic volumes. Based on INRIX bottleneck ranking tool, SB direction of US 29 is listed as one of the highly congested corridors.

After converting the raw data to volumes, it was determined that ATSPM data from this corridor would not be supportive in validating the demand estimation methods. This was due to missing data and unrealistic noise observed in the volumes. First, no sensor data were available for April 2021 for the downstream intersections 5 and 6. The same was true for sensors on SB through movements at intersection 2. As shown in Figure 8, the volume for this intersection is close to zero. Second, the volumes exhibited unrealistic fluctuations after April 12, especially those of intersections 1 and 3.

Even though the evaluated ATSPM sample data did not prove to be useful for this project to provide the ground truth volumes, it should be mentioned that ATSPM data have potential to support various traffic analyses needs. Additional work is needed to evaluate the quality of the ATSPM data and streamline its usage in various applications. Since this was beyond the scope of this research project, further investigation of the ATSPM data for validating the demand estimation methods was left for a future study.

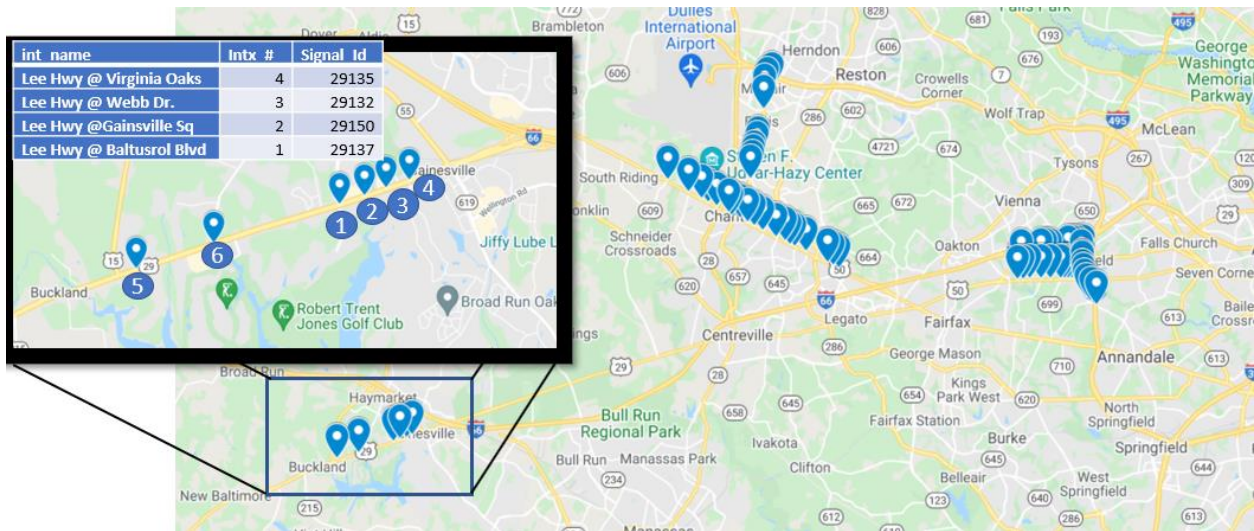


**Figure 7. Intersections with ATSPM data in Northern Virginia**

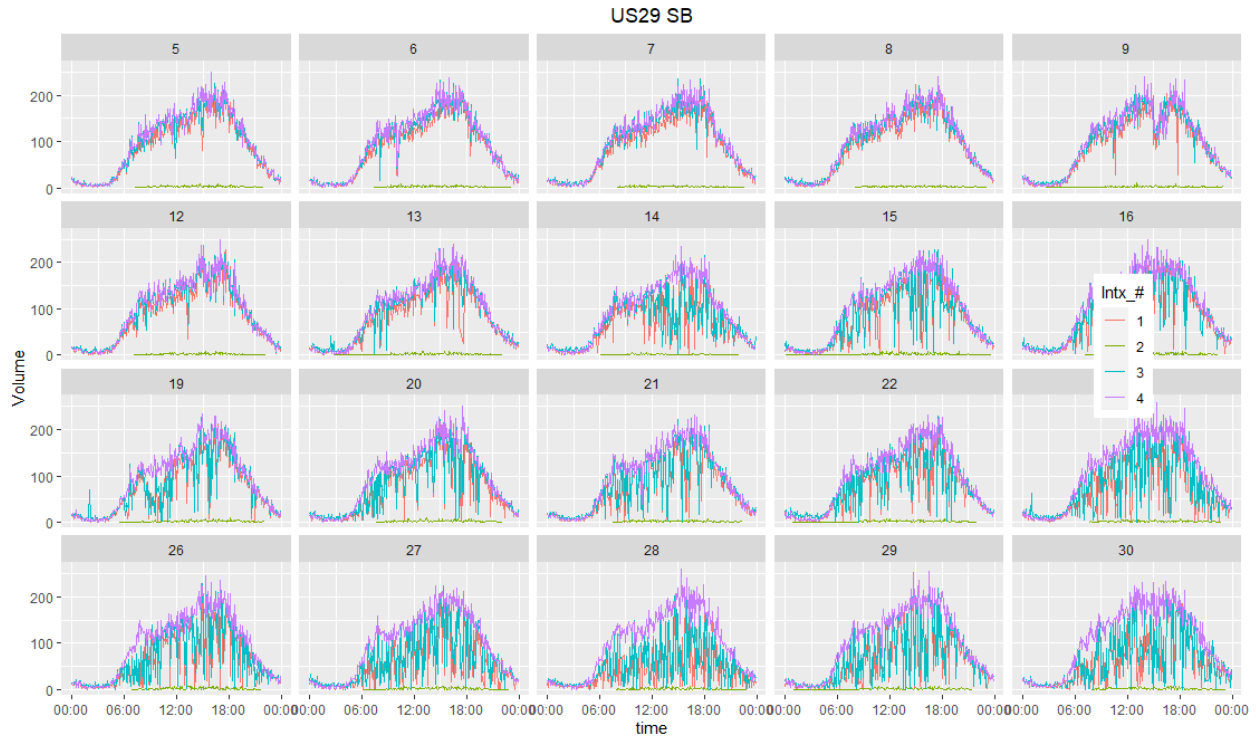


**Figure 8. Five-minute volume profiles for the SB movements of four intersections on US 29 extracted from the ATSPM data for weekdays in April 2021. Numbers above the plots refers to the day of the month in April 2021. The names of the intersections can be found in the inset in Figure 7.**

To collect ground truth volume data for an oversaturated corridor, the team selected the Indian River Road (IRR) corridor in the City of Virginia Beach based on the speed profiles from the INRIX data. The eastbound direction between I-64 and Kempsville Road is generally oversaturated in weekdays in the afternoon hours. The XD segment from Centerville Turnpike to Ferry Point Road/Thompkins Lane (see Figure 9) is selected for volume data collection. This segment is about 0.33 mi. Video cameras were installed at the upstream and downstream ends of this segment in the afternoon hours on three days in September: 21<sup>st</sup>, 22<sup>nd</sup> and 28<sup>th</sup>. The cameras were attached to poles on the sidewalk and removed after the data collection was complete on each day.

Post processing of the video was done by manual methods for the most part. Volume data were extracted and reported for each cycle as shown in the Appendix. These volume counts were used in model validation described in Results section. The video collected on Sept 28<sup>th</sup> was also processed through a custom vehicle detection program developed by this Old Dominion University (ODU) research team for a different project. The program's image-processing algorithms detect and track vehicles in the video and attach a timestamp when each vehicle is detected (see Figure 10). These timestamps were used to create cumulative plots to visualize the variation in flow rate over time (shown in the Results section). The counts from the video image processing method matched the data from the manual method reasonably well: the mean absolute percentage error was about 4%.

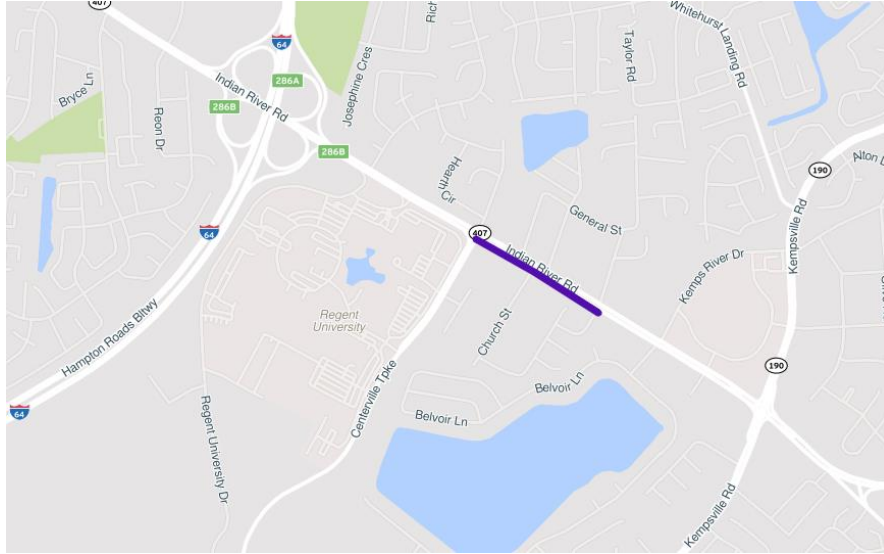


**Figure 9. The INRIX XD segment on Indian River Road selected for volume data collection**



**Figure 10. Sample images from the vehicle detection program**

## RESULTS

### Literature Review

There are different approaches to quantify the demand depending on the type of method and technology being used. Several existing intelligent transportation systems technologies, including inductive loop detectors, video cameras, sensors, unmanned aerial vehicles (UAVs), CVs, probe vehicles, etc., may support the estimation of the demand volume. Various supporting methods are proposed to estimate demand volume using data from these technologies such as queue estimation methods, volume delay functions (VDFs), speed, delay and travel time studies and predictive data analytics. Each of these methods along with the technologies used by them was evaluated based on the available literature, and the findings are summarized in the following paragraphs.

## **Demand Volume Estimation Based on Vehicle Detection Sensors**

Queue estimation methods form the backbone of the demand volume estimation process for oversaturated conditions. If the maximum queue lengths are accurately predicted, the demand volume arriving at the back of the queue can be determined by employing the conservation of vehicles principle or an input-output method. One such model is first proposed by Berry in his 1987 paper that computes the arrival volume in a cycle as a sum of the departing volume and the residual queue at the end of that cycle minus the residual queue in the preceding cycle (Berry, 1987). The departing volume can easily be counted by sensors at the intersection. Measuring the residual queue at the end of each cycle is more challenging, as the queue can grow to an arbitrary length. Therefore, the success of this method hinges on an accurate way to observe the maximum queue length under oversaturated conditions. Unfortunately, the current queue estimation methods in the literature are not effective for estimating the queue beyond the upstream detector. Moreover, detector data is prone to noise and detector failures (Islam, 2013).

A few researchers have suggested the use of magnetic sensors and signature matching for finding link volumes (Papageorgiou and Varaiya, 2009; Li et al., 2017). Another method for estimating queue length has been proposed in which queue length can be estimated up to five to ten times greater than the distance between the detector and the stop line (Mück, 2002) but the main limitation of that approach is the assumption of a constant arrival rate of vehicles (Liu et al., 2009). While these methods seem promising in estimating the demand volume using the input-output model, they need further analysis to be applied under oversaturated conditions.

Other methods based on shockwave theory and the detector technology have also been explored in the literature. In one method, congestion due to oversaturation and spillbacks can be easily identified, but the maximum queue length cannot be exactly estimated -- especially when the queue is very long. This is because the vehicles in queue do not cross the advanced detector even after the signal turns green (Wu et al., 2010). In another method, Cho et al. (2014) applied shockwave theory to estimate the volume and speed in the upstream of the signal under oversaturated conditions. However, both of these methods require the use of at least two detectors, one of which must be an advanced detector at a considerable distance from the intersection, which may not be practical. To implement the second method, effective solutions are needed to detect the propagation of shockwaves from sensor data (Cho and Tseng, 2007; Yao and Tang, 2019).

## **Probe Vehicle or CV Data for Estimating Queue Dynamics and Volume**

Rather than relying on fixed sensors, queuing dynamics can be observed more directly from trajectory data of probe vehicles. To the best of our knowledge, the first study on estimating queue lengths at signalized intersections using probe vehicle data was conducted by Comert and Cetin (2009). They assumed a point queue model and Poisson arrivals to derive statistical models to estimate the queue length. The error in the estimation of queue length is a function of the market penetration rate of the probe vehicles in the traffic stream. However, their proposed statistical model is not applicable to oversaturated conditions.

To accommodate oversaturated conditions, Cetin (2012) proposed a shockwave theory-based method for estimating the back of the queue profile from the known positions of probe vehicles when they first join the back of the queue. Based on data from a VISSIM simulation, the proposed model is shown to predict the back of the queue profile reasonably well even at low market penetration rates (e.g., 5 to 10%) and in the absence of probes in some cycles (Cetin, 2012). Although this model works efficiently for single lane queues, it would need further development to work for multilane scenarios and requires raw probe data (i.e., GPS position and time) as the input.

Similar studies have been conducted by Ramezani and Geroliminis (2013, 2015), who were also able to estimate queue length under oversaturated conditions limited to a single lane. They have suggested further improvements in terms of accommodating multi-lane analysis, precisely locating the probe vehicles, lane identification, and data fusion between detectors and probes. Cheng et al. (2011) have also provided a method to estimate cycle-by-cycle queue length using GPS location data from the probes. Ban et al. (2011) proposed a method to estimate queue lengths using travel time data from mobile sensors, but their method was not tested under oversaturated conditions.

Zhang et al. (2019) also proposed a method to estimate the back of the queues using an Expectation Maximization approach when the Market Penetration (MP) of probe trajectories is low. Tan et al. (2021) used a Maximum Likelihood Estimation approach to estimate the same with sparse probe vehicle data. Both these methods still need signal timing data and are applicable to through lanes only. These models seem promising but need improvement on their application to mixed lane analysis, queue spillbacks, and real time applications (Zhao et al., 2019). Methods which infer vehicles between probe vehicles can also be implemented to improve estimations but have not been evaluated for unevenly distributed lane volumes or oversaturation conditions (Cetin and Anuar, 2017; Salahshour et al., 2019).

The development of CV technology can reduce the dependency on the conventional detectors. Luo et al. (2019) have provided a method to estimate the traffic volume along with delays using Vehicle to Cloud communication, even at a low MP of 10%. However, their method is dependent on Vehicle to Cloud communication infrastructure (Luo et al., 2019). Zheng (2016) and Zheng and Liu (2017) employed Vehicle to Infrastructure communication to estimate the traffic volume and other parameters with reasonable accuracy at low MP of 10%, but their method is not suitable for oversaturated conditions. Gao et al. (2019) have used Vehicle to Everything communication and the back propagation neural network approach to estimate queue lengths even in a mixed traffic environment. Gao et al. (2020) also applied a Deep Neural Network method which replaces shockwave theory approach to estimate queues using Internet of Things technology. These approaches seem promising as they reduce the dependency on detectors. Shahrabaki et al. (2018) combined the data from both detectors and CVs using V2I communication to estimate the traffic flow. However, their method requires high resolution data from the upstream detector. Ma and Qian (2019) used AV (Automated Vehicle) technology for traffic sensing and to estimate traffic parameters like speed, density, and flow even under low MP rates. If probes are provided with this technology, they can help in estimating traffic parameters accurately. But all the above methods still need to be improved further for their application to oversaturated traffic conditions.

## **Demand Volume Estimation Using VDFs and Travel Time-Flow Relationships**

The relationship between flow and travel time was established by Davidson in 1966, and since then many researchers have explored this relationship (Davidson, 1966). For example, Taylor (1977) proposed a new method to estimate the parameters of the Davidson flow-travel time relationship. Both methods are not applicable for oversaturated conditions. Akçelik provided an alternative travel time function and a time dependent form of Davidson's function to overcome the problems associated with parameter tuning and his model is applicable to oversaturated conditions (Akçelik, 1991).

Link performance functions used in the travel demand models can be used to estimate the demand beyond the capacity when locally calibrated. Huntsinger and Rouphail (2011) have successfully applied this technique to estimate the demand under oversaturation on freeways. Their method used a simple approach where actual demand is the sum of demand at capacity plus the queue length. Therefore, finding the queue length on freeways or on arterials plays an important role in the estimation of the demand under any traffic condition. However, Huntsinger and Rouphail's method is applicable only for freeway corridors.

Cetin et al. (2012) have observed that calibrating VDFs based on link travel time or speed does not yield accurate results in Travel Demand Model applications and, therefore, proposed a link count based Genetic Algorithm approach to calibrate optimal VDF parameters under congested conditions. Foytik et al. (2013) calibrated the Bureau of Public Roads function using a similar Genetic Algorithm approach using link counts and found that VDFs calibrated to high demand perform well under variable demand as well. Their method is tailored to a network-level calibration needed in Travel Demand Models and may not be applicable to calibrating VDFs for a given corridor.

Kucharski and Drabicki (2017) proposed the estimation of a VDF based on density instead of flow and found their performance is more realistic. So et al. (2017) have created the So-Stevanovic VDF which is claimed to be better than the BPR function by linking the VDFs with upstream travel times for  $v/c$  ratio estimation at an isolated intersection. Nevertheless, their method is not directly applicable to oversaturated conditions.

Moses et al. (2013) have worked on calibrating VDFs based on speed-flow data and found that more than one VDF is required to achieve the desired forecasting accuracy in urban regions. They also conducted a study on various VDFs and found that the Akçelik function is suitable for urban streets and the modified Davidson function performed well on all facilities (Mtoi and Moses, 2014). Utilizing speeds for volume or demand estimation needs to be explored further.

Hao et al. (2013) have utilized travel times to estimate vehicle indices which are closely associated with vehicle arrival and departure processes. Morgul et al. (2014) have proposed the use of virtual sensors in a web-based approach to estimate the travel times. Moreover, Yang et al. (2015) have provided an improved travel time estimation for closed highways. However, all these methods are applicable only for travel time estimation and do not estimate demand under oversaturated conditions.

## **Video Image Processing and Unmanned Aerial Vehicles (UAVs) for Estimating Volume**

Video data processing has been considered as a means of overcoming the shortfalls of conventional detector technologies in demand estimation. Researchers have been exploring video detection for extracting volumes, speeds, and other traffic flow parameters. Coifman et al. (1998) developed algorithms for tracking vehicles from video image data under challenging conditions like occlusion, shadows, lighting transitions, and congestion. Ma et al. estimated lane-wise traffic demand (Ma et al. 2017) and queue lengths (Ma et al., 2018) using virtual detectors called video imaging detectors. Their model needs improvement in accuracy to detect traffic under oversaturated conditions. Luo et al. (2019) estimated queue lengths by applying the license plate recognition method to the video images but did not consider queue spillbacks. Li et al. (2019) estimated traffic volumes only in undersaturated conditions. Although Zhang et al. (2020) were able to predict the trajectory of vehicles using the LPR method and video imaging, their model is also not suitable for oversaturated conditions.

Researchers have also utilized and proposed various machine learning and computer vision techniques to process image data from UAVs. Khan et al. (2018) proposed an analytical method for shockwave identification and estimation of traffic parameters like density at signalized intersections using UAV images. Khan et al. also developed a universal guiding framework for UAV-based traffic analysis (Khan et al., 2017a) and for automated multivehicle trajectory extraction (Khan et al., 2017b). Ke et al. (2020) created an advanced framework for estimating microscopic lane level traffic parameters from UAV video, which needs further development for real-time applications. Wang (2016) explained a method for collecting and processing the data using the UAVs. Kim et al. (2019) extracted vehicle trajectories using the Faster Region-based Convolutional Neural Network method from UAV images. Furthermore, Feng et al. (2020) proposed a method to extract trajectory data using UAVs under mixed traffic conditions using the Convolutional Neural Network technique. Zhu et al. (2018) have estimated traffic density by applying the Deep Neural Network method and using UAV data. Moreover, Jian et al. (2019) used UAVs for identification of traffic congestion on roads. Khan et al. (2020) also worked on smart traffic monitoring using UAVs. Yahia et al. (2019) also proposed methods based on Kalman filtering to identify traffic congestion as well as to estimate traffic flow using UAVs. Babinec and Apeltauer (2016) worked on accurately estimating the position of vehicles using UAVs. Barmounakis et al. (2016) and Barmounakis and Geroliminis (2020) used Unmanned Aerial Aircraft Systems (UAS) and massive drone data for traffic surveillance and monitoring.

The use of UAVs for traffic analysis seems to have been gaining momentum in recent years and will play a significant role as UAVs become more common due to their other capabilities, including security monitoring and commercial service deliveries. However, deployment of this technology is currently costly for large scale deployment. Therefore, an effective methodology is needed for estimating demand volume for oversaturated corridors based on readily available data from existing or widely deployed intelligent transportation systems technologies.

## Application of the Demand Estimation Methods Using Simulation Data

The two demand estimation methods discussed previously were applied to the simulation data generated for the two-lane road network and the IRR network. The results are discussed in the next two subsections.

### Results for the Simulated Two-Lane Road Network

The simulated data were processed to generate the speed profiles shown in Figure 11 for the eight TMC lengths (ranging from 250 meters to 2000 meters) considered. In Figure 11, it is apparent that the average speed values drop considerably and become stable after the critical times  $t_2$  – indicated on the charts with vertical red lines. After these critical times, the queue covers the entire TMC segment length and, hence, causes the speeds to remain low. This phenomenon is explained previously in the methods section in the context of field data shown Figure 1. For each scenario, these critical times along with other inputs needed for the two demand estimation methods are extracted from the trajectory and simulated TMC speed data.

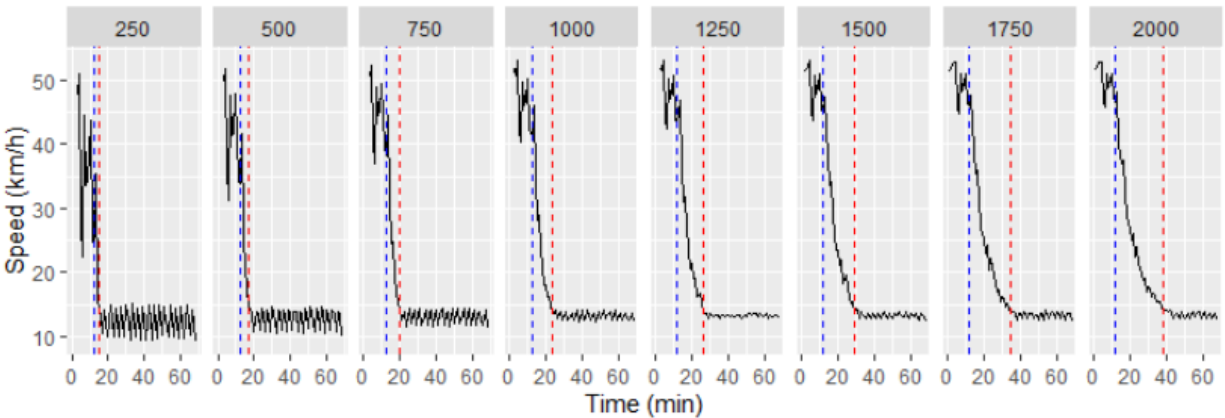


Figure 11. Speed profiles created from VISSIM data for different simulated TMC lengths ranging from 250 meters to 2000 meters (numbers shown at the top of each plot). The red dashed lines indicate  $t_2$ , the times when the queue starts completely covering the TMC segment. The blue dashed lines indicate the times when the oversaturated period begins.

For the SW method, the extracted parameters and the model results are shown in Table 1 and results for the VDF method are in Table 2. The parameters shown in these two tables are explained below.

- Sim. Run#: The simulation model is run three times (by changing the random number seed in VISSIM) to account for random variations due to vehicle speeds, arrival times, and other stochastic elements within VISSIM. This column shows the simulation run number.
- Length: This refers to the simulated TMC length.
- T: This corresponds to the difference between  $t_2$  and  $t_1$  (i.e.,  $T = t_2 - t_1$ ) which captures how long it takes for the queue to reach the beginning of the TMC segment. For each case,  $t_1$  is set to 12 minutes since within the 12<sup>th</sup> minute, the input flow rate with 2,400 vehicles/hour reaches the traffic signals. The critical time  $t_2$  is computed from the speed profiles shown in Figure 11.

- $U_A$ : For the SW method, this is simply the free-flow speed in the network as vehicles approach the back of the queue with FFS. For the VDF method, this is computed as the average speed from TMC speed profiles from the observations before  $t_1$ .
- $U_C$ : For both methods, this is the average of all TMC speeds after  $t_2$ , i.e., the average speed within the queue.
- $q_C$  or  $c$ : This refers to the queue discharge rate, which is equivalent to the capacity of the intersection in this case.
- Est  $q_A$ : This is the estimated demand volume computed from the equations presented earlier (Equation 2 for the SW method and Equation 4 for the VDF method).
- Obs  $q_A$ : This refers to the flow rate computed based on the actual arrivals within the period  $T$ . Even though the arrival rate (demand volume) is 2,400 vehicles/hour, due to the random generation of the vehicles in VISSIM, the actual flow rate fluctuates over the simulation time. Therefore,  $q_A$  is taken as the observed flow rate rather than the input flow rate.
- $k$  and  $I$ : For the VDF method, these two parameters are looked up from HCM 2000 tables as indicated before.
- Obs Delay: For the VDF method, this corresponds to the average delay per vehicle and is calculated as shown in Equation (5).
- $X$ : This is the volume/capacity ratio in the HCM VDF equation.
- % Err: Percent error is computed as  $(\text{Est } q_A - \text{Obs } q_A) / \text{Obs } q_A \times 100$ .

From the results presented in Table 1 and Table 2, it is observed that both methods yield reasonably accurate estimates for the demand volume. The mean absolute percentage errors were calculated to be 2.5% and 2.8% for the SW and VDF methods respectively. The error is higher when the TMC segment length is short. This can be attributed to the relatively short observation interval  $T$  for shorter segments. For the 250-meter scenarios,  $T$  is only several minutes. Measuring traffic flow or counts within such short intervals typically results in a large variation. Furthermore, since the time resolution is one minute, the precision of estimating event times (e.g.,  $t_2$  and  $t_1$ ) is only accurate within  $\pm$  one minute. This plays a larger role when  $T$  (or the TMC segments) are short. Figure 12 shows the average error across the three simulation runs for the two methods as the TMC length is varied.

**Table 1. Parameters for the SW method and the estimated volume demands under different scenarios**

Sim. Run#	Length (km)	T (min)	U <sub>A</sub> (km/h)	U <sub>C</sub> (km/h)	w (km/h)	q <sub>c</sub> (vph)	Est q <sub>A</sub> (vph)	Obs q <sub>A</sub> (vph)	% Err
1	0.25	2	51.0	12.3	-7.5	1,993	2,795	2,838	-1.5%
1	0.50	5	51.0	12.8	-6.0	1,993	2,618	2,698	-3.0%
1	0.75	7	51.0	12.9	-6.4	1,993	2,651	2,688	-1.4%
1	1.00	10	51.0	13.0	-6.0	1,993	2,605	2,656	-1.9%
1	1.25	11	51.0	13.1	-6.8	1,993	2,673	2,644	1.1%
1	1.50	14	51.0	13.2	-6.4	1,993	2,634	2,586	1.9%
1	1.75	20	51.0	13.2	-5.3	1,993	2,528	2,537	-0.4%
1	2.00	23	51.0	13.2	-5.2	1,993	2,525	2,509	0.6%
2	0.25	4	51.0	12.3	-3.8	1,993	2,423	2,577	-6.0%
2	0.50	5	51.0	12.8	-6.0	1,993	2,619	2,544	3.0%
2	0.75	8	51.0	13.0	-5.6	1,993	2,573	2,546	1.1%
2	1.00	11	51.0	13.2	-5.5	1,993	2,546	2,414	5.5%
2	1.25	17	51.0	13.1	-4.4	1,993	2,450	2,430	0.8%
2	1.50	22	51.0	13.2	-4.1	1,993	2,418	2,434	-0.7%
2	1.75	23	51.0	13.2	-4.6	1,993	2,462	2,436	1.1%
2	2.00	26	51.0	13.2	4.6	1,993	2,465	2,423	1.7%
3	0.25	3	51.0	12.3	-5.0	1,993	2,553	2,754	-7.3%
3	0.50	5	51.0	12.9	-6.0	1,993	2,615	2,660	-1.7%
3	0.75	8	51.0	13.0	-5.6	1,993	2,570	2,561	0.3%
3	1.00	11	51.0	13.2	-5.5	1,993	2,546	2,515	1.2%
3	1.25	14	51.0	13.2	-5.4	1,993	2,535	2,536	0.0%
3	1.50	17	51.0	13.3	-5.3	1,993	2,525	2,494	1.2%
3	1.75	23	51.0	13.3	-4.6	1,993	2,458	2,446	0.5%
3	2.00	26	51.0	13.4	-4.6	1,993	2,457	2,432	1.0%

**Abbreviations used in the table:**

Sim. Run #	- Simulation run number
Length	- Length of the segment in km
T	- The time it takes for the speed to drop from free flow speed to congested speed
U <sub>A</sub>	- Speed under free flow condition in km/hr
U <sub>C</sub>	- Speed under congestion (or oversaturation) in km/hr
w	- Shockwave speed
q <sub>c</sub>	- Maximum flow (capacity) across intersection observed from simulation in vph
vph	- vehicles per hour
Est q <sub>A</sub>	- Estimated arrival rate of vehicles in vph
Obs q <sub>A</sub>	- Observed arrival rate of vehicles in vph
% Err	- Percentage error between the estimated and the actual arrival rates

**Table 2. Parameters for the VDF method and the estimated volume demands under different scenarios**

Sim. Run #	Length (km)	T (min)	I	k	U <sub>A</sub> km/h	U <sub>C</sub> km/h	Obs Delay (s)	c (vph)	X	d <sub>2</sub> (s)	Est q <sub>A</sub> (vph)	Obs q <sub>A</sub> (vph)	% Err
1	0.25	2	1	0.5	30.9	12.3	22.0	1,993	1.31	21.9	2,613	2838	-7.9%
1	0.50	5	1	0.5	38.5	12.8	46.9	1,993	1.29	46.8	2,565	2698	-4.9%
1	0.75	7	1	0.5	42.0	12.9	72.5	1,993	1.33	72.4	2,647	2688	-1.5%
1	1.00	10	1	0.5	45.3	13.0	98.6	1,993	1.32	98.5	2,624	2656	-1.2%
1	1.25	11	1	0.5	46.5	13.1	123.4	1,993	1.36	123.3	2,718	2644	2.8%
1	1.50	14	1	0.5	47.1	13.2	147.8	1,993	1.34	147.7	2,678	2586	3.5%
1	1.75	20	1	0.5	47.6	13.2	173.3	1,993	1.28	173.2	2,555	2537	0.7%
1	2.00	23	1	0.5	48.9	13.2	199.9	1,993	1.28	199.9	2,559	2509	2.0%
2	0.25	4	1	0.5	31.1	12.3	221	1,993	1.14	22.0	2,266	2577	-12.1%
2	0.50	5	1	0.5	38.4	12.8	46.9	1,993	1.29	46.8	2,565	2544	0.8%
2	0.75	8	1	0.5	41.8	13.0	71.8	1,993	1.28	71.7	2,556	2546	0.4%
2	1.00	11	1	0.5	44.9	13.2	96.5	1,993	1.28	96.4	2,551	2414	5.7%
2	1.25	17	1	0.5	46.0	13.1	122.2	1,993	1.23	122.1	2,452	2430	0.9%
2	1.50	22	1	0.5	47.0	13.2	147.7	1,993	1.22	147.6	2,424	2434	-0.4%
2	1.75	23	1	0.5	48.2	13.2	173.3	1,993	1.24	173.2	2,480	2436	1.8%
2	2.00	26	1	0.5	48.5	13.2	197.7	1,993	1.25	197.7	2,487	2423	2.6%
3	0.25	3	1	0.5	35.3	12.3	23.9	1,993	1.22	23.8	2,428	2754	-11.8%
3	0.50	5	1	0.5	41.6	12.9	48.3	1,993	1.30	48.2	2,585	2660	-2.8%
3	0.75	8	1	0.5	44.6	13.0	73.3	1,993	1.29	73.2	2,569	2561	0.3%
3	1.00	11	1	0.5	46.8	13.2	98.2	1,993	1.29	98.2	2,562	2515	1.9%
3	1.25	14	1	0.5	47.8	13.2	123.2	1,993	1.28	123.1	2,558	2536	0.9%
3	1.50	17	1	0.5	48.5	13.3	147.6	1,993	1.28	147.5	2,554	2494	2.4%
3	1.75	23	1	0.5	49.3	13.3	173.2	1,993	1.24	173.1	2,480	2446	1.4%
3	2.00	26	1	0.5	49.7	13.4	196.3	1,993	1.25	196.3	2,483	2432	2.1%

**Abbreviations used in the table:**

Sim. Run #	- Simulation run number
Length	- Length of the segment in km
T	- The time it takes for the speed to drop from free flow speed to congested speed
I	- Upstream filtering/metering adjustment factor
k	- Incremental delay factor that is dependent on controller settings
U <sub>A</sub>	- Speed under free flow in km/hr
U <sub>C</sub>	- Speed under congestion in km/hr
Obs Delay	- Observed delay in seconds
c	- Maximum flow (capacity) across intersection observed from simulation in vph
vph	- Vehicles per hour
X	- Lane group v/c ratio or degree of saturation
d <sub>2</sub>	- Incremental delay
Est q <sub>A</sub>	- Estimated arrival rate of vehicles in vph
Obs q <sub>A</sub>	- Observed arrival rate of vehicles in vph
% Err	- Percentage error between the estimated and the actual arrival rates

From the results presented in Figure 12, the average error rates (calculated from the three simulation runs) are within approximately  $\pm 2\%$  when TMC length is 500 meters or longer. While these error rates look promising, in real life applications with field data, larger errors might occur

due to additional uncertainties. For example, travel speeds reported by INRIX (or any other data source) may exhibit more variance and uncertainty due to a low probe vehicle sample size, variation in travel speeds across different travel lanes, and complex traffic conditions (e.g., bus stops and slow-moving trucks).

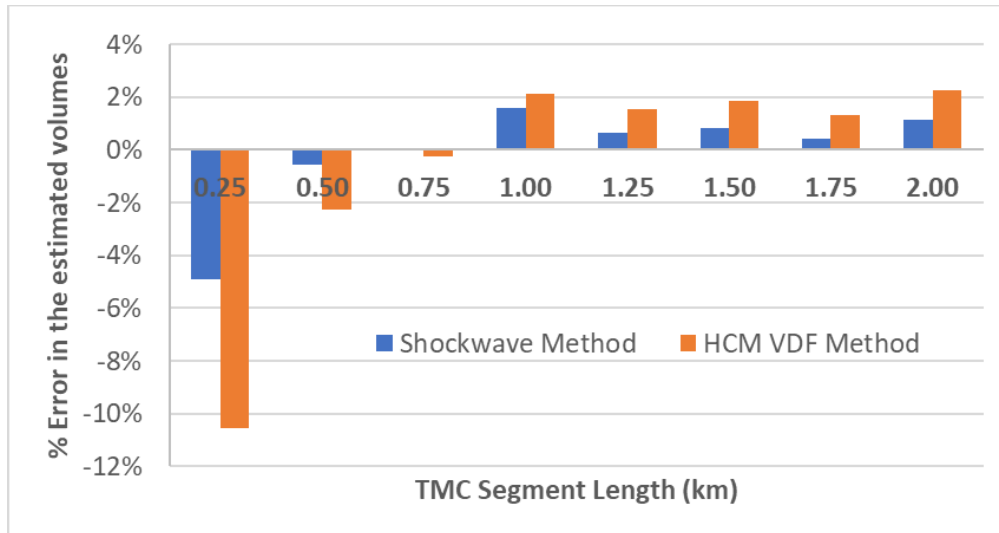


**Figure 12. Average errors in estimating demand volume from the SW and VDF methods that are computed from the results of three simulation runs as TMC segment length is varied**

### Results for the Simulated IRR Network

For the IRR network, four different demand levels were simulated (see Figure 6 for the demand profiles). Each demand scenario was simulated three times in VISSIM with different random number seeds. It is observed that a queue starts forming upstream of the Regent University Dr. intersection a few minutes after the 20th minute, the time when the demand peaks. After processing the vehicle trajectories within each XD segment, average speed profiles were created. Sample XD speed profiles for one of the scenarios are shown in Figure 13. XD5 is directly upstream of the signalized intersection. Average speeds at this segment are low even when the demand is below the peak value. The speeds for the remaining XD segments (1 to 4) in the upstream of the bottleneck are initially at around the FFS (free-flow speed) of 55 km/h as they are not impacted by queuing at the signals when the demand is low. After the peak demand is loaded, the queue grows and eventually reaches to the other four segments.

As shown previously in Figure 5, the lengths of the XD segments are relatively short (segments 1-4 are shorter than 250 meters). Since these XD segments are short, estimating the SW speed from an individual speed profile will not be very reliable as explained in the previous section. Therefore, the propagation speed of the queue was estimated using data from multiple segments. Based on the profiles in Figure 13, it can be inferred that the queue has reached the beginning of XD4 at the 25th minute and that of XD1 at the 30th minute. The sum of the lengths of XD1, XD2, and XD3 is 590 m. In this example, the SW takes 5 minutes to travel 590 meters. This observation is used to estimate the SW speeds. These speeds are reported in Table 3 along with other inputs data for the SW method.

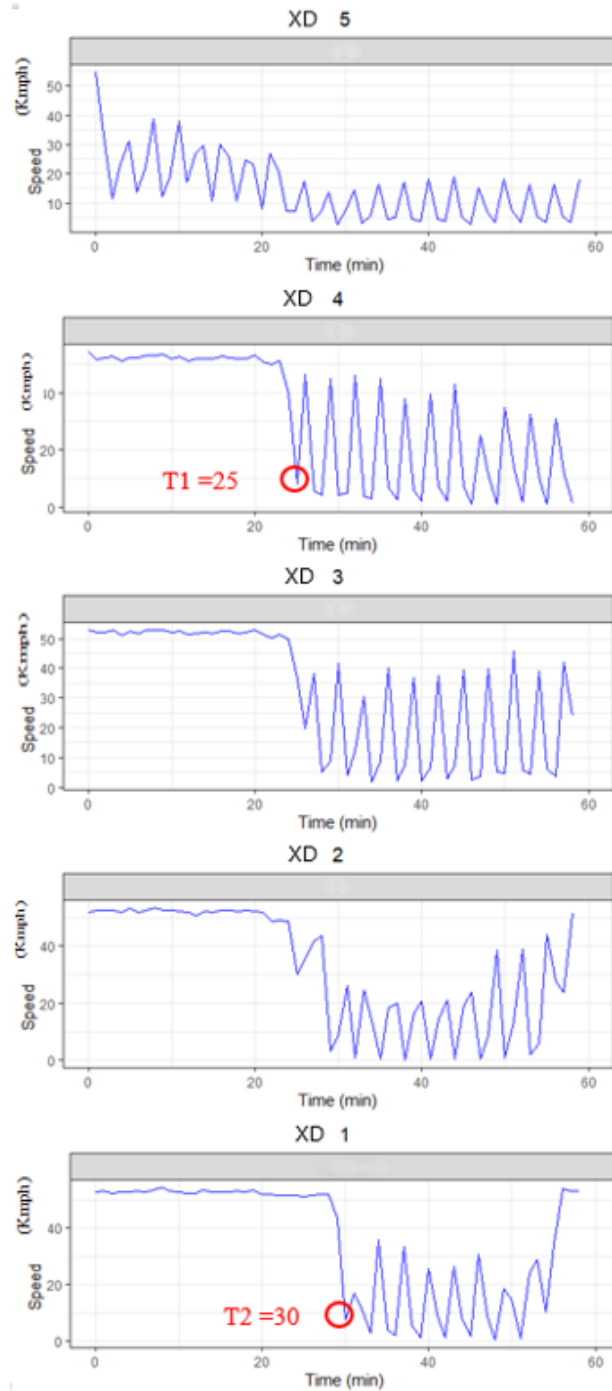


**Figure 13. Speed profiles for the simulated XD segments in the IRR network**

The demand volumes loaded onto the network on the mainline and ramps are shown in Table 3. For the first three scenarios, the ramp volumes are low (i.e., 100 vehicles/hour) and all ramp vehicles can merge onto IRR without causing a queue on the ramp. For the last scenario, the demand from Ramp-2 is 1,000 vehicles/hour and results in a backup on the ramp. During the congested period, vehicles can enter from this ramp onto IRR at 720 vehicles/hour. The column ‘Ramp Inflow’ gives the total ramp volume entering the IRR corridor. The total demand volume

for the IRR is then the sum of ramp inflow and mainline flow (this sum is shown in Table 4 as Obs  $q_A$ ). This sum is what the demand estimation methods attempt to predict.

Table 3 and Table 4 summarize the results of the SW and VDF methods respectively. The estimated demand volumes (indicated by Est  $q_A$ ) are compared to the demand volumes entering the network (shown in Table 4 as Obs  $q_A$ ). The percent errors are reported for each simulation run as well as for the given demand scenarios as an average of three runs. As expected, these error rates are higher than those shown in Table 1 and Table 2 for the two-lane road network. This can be attributed to the relatively more complex geometry and traffic flow on the IRR network. Furthermore, in the two-lane network case, the estimated volumes are compared to the observed flow rates in simulation (within time T) rather than the input flow rates. Due to the randomness in vehicle generation process in VISSIM, the flow rate in a given period would not be equal to the loaded demand rate but would fluctuate around it.

The results shown in Table 3 and Table 4 demonstrate both methods produce relatively accurate results. The errors for the VDF method are a bit lower. The mean absolute percentage errors are 5.4% and 4.2% for the SW and VDF methods respectively.

**Table 3. Parameters for the SW method and the estimated volume demands for the simulated IRR network**

Sc #	Sim. Run #	Loaded Demand (vph)				$t_1$	$t_2$	T (min)	w km/h	$U_c$ km/h	Est $q_A$ (vph)	% Err	Avg. Err
		Main	Ramp 1	Ramp 2	Ramp Inflow								
1	1	3,500	100	100	200	28	36	8	-4.4	16	3,722	1%	4%
	2	3,500	100	100	200	27	33	6	-5.9	15	3,964	7%	
	3	3,500	100	100	200	30	36	6	-5.9	16	3,894	5%	
2	1	4,000	100	100	200	25	30	5	-7.1	16	4,026	-4%	-4%
	2	4,000	100	100	200	28	33	5	-7.1	15.5	4,065	-3%	
	3	4,000	100	100	200	25	30	5	-7.1	16	4,026	-4%	
3	1	4,500	100	100	200	25	29	4	-8.9	16	4,214	-10%	-9%
	2	4,500	100	100	200	23	27	4	-8.9	15	4,314	-8%	
	3	4,500	100	100	200	25	29	4	-8.9	15.75	4,238	-10%	
4	1	4,000	100	1,000	<b>820</b>	25	29	4	-8.9	10.85	4,927	2%	-2%
	2	4,000	100	1,000	<b>820</b>	22	27	5	-7.1	10.85	4,612	-4%	
	3	4,000	100	1,000	<b>820</b>	24	29	5	-7.1	10.5	4,673	-3%	

**Abbreviations used in the table:**

- Sc # : Demand scenario number
- Sim. Run # : Simulation run number
- $t_1$  : The time when the oversaturation is estimated to begin based on the speed profiles
- $t_2$  : The estimated time at which the queue reaches the beginning of the TMC segment
- T :  $t_2 - t_1$  or the time it takes for the speed to drop from free flow speed to congested speed
- w : Speed of the shockwave produced due to queuing under congestion
- $U_c$  : Speed under congestion in km/hr
- vph : Vehicles per hour
- Est  $q_A$  : Estimated arrival rate of vehicles (or demand volume)
- % Err : Percentage error of the estimated demand volume
- Avg.Err : Average of the three percentage errors in each demand scenario

**Table 4. Parameters for the VDF method and the estimated volume demands for the simulated IRR network**

Sc #	Sim Run#	L (km)	T (min)	I	k	U <sub>A</sub> (km/h)	U <sub>C</sub> (km/h)	Obs Delay (s)	c (vph)	x	d <sub>2</sub> (s)	Est q <sub>A</sub> (vph)	Obs q <sub>A</sub> (vph)	% Err	Avg. Err
1	1	0.59	8	1	0.5	55.0	16.0	47.1	3,150	1.18	47.1	3,723	3,700	1%	5%
	2	0.59	6	1	0.5	55.0	15.0	51.5	3,150	1.27	51.5	4,007	3,700	8%	
	3	0.59	6	1	0.5	55.0	16.0	47.1	3,150	1.25	47.1	3,926	3,700	6%	
2	1	0.59	5	1	0.5	55.0	16.0	47.1	3,150	1.30	47.1	4,089	4,200	-3%	-2%
	2	0.59	5	1	0.5	55.0	15.5	49.2	3,150	1.31	49.3	4,137	4,200	-1%	
	3	0.59	5	1	0.5	55.0	16.0	47.1	3,150	1.30	47.1	4,089	4,200	-3%	
3	1	0.59	4	1	0.5	55.0	16.0	47.1	3,150	1.38	47.1	4,333	4,700	-8%	-7%
	2	0.59	4	1	0.5	55.0	15.0	51.5	3,150	1.41	51.5	4,451	4,700	-5%	
	3	0.59	4	1	0.5	55.0	15.8	48.1	3,150	1.38	48.1	4,361	4,700	-7%	
4	1	0.59	4	1	0.5	55.0	10.9	78.6	3,150	1.64	78.6	5,175	4,820	7%	2%
	2	0.59	5	1	0.5	55.0	10.9	78.6	3,150	1.51	78.6	4,765	4,820	-1%	
	3	0.59	5	1	0.5	55.0	10.5	81.8	3,150	1.53	81.8	4,835	4,820	0%	

**Abbreviations used in the table:**

- Sc # - Demand scenario number
- Sim. Run # - Simulation run number
- L - Length of the segment in km
- T - the time it takes for the speed to drop from free flow speed to congested speed
- I - Upstream filtering/metering adjustment factor
- k - Incremental delay factor that is dependent on controller settings
- U<sub>A</sub> - Speed under free flow in km/hr
- U<sub>C</sub> - Speed under congestion in km/hr
- Obs Delay - Observed Delay in seconds
- C - Maximum flow (Capacity) across intersection observed from simulation in vph
- vph - Vehicles per hour
- X - Lane group v/c ratio or degree of saturation
- d<sub>2</sub> - Incremental delay
- Est q<sub>A</sub> - Estimated arrival rate of vehicles in vph
- Obs q<sub>A</sub> - Observed arrival rate of vehicles in vph
- % Err - Percentage error between the estimated and the actual arrival rates in simulation
- Avg.Err - Average of the three percentage errors in each demand scenario

**Validation of the Methods on the Field Data**

The SW and VDF methods were tested with the field data collected on IRR on September 21<sup>st</sup>, 22<sup>nd</sup>, and 28<sup>th</sup> 2021. For each one of these days, INRIX XD data were analyzed to determine the critical times  $t_1$  and  $t_2$ . These are shown in Figure 14 on INRIX speed profiles. For Sept 28<sup>th</sup>, there are two occasions of oversaturation observed within the video data collection period. As seen in Figure 14, speeds go back to around 30 mph between 4:30 PM and 5:30 PM twice. This gives the opportunity to apply the model twice to Sept 28<sup>th</sup> data.

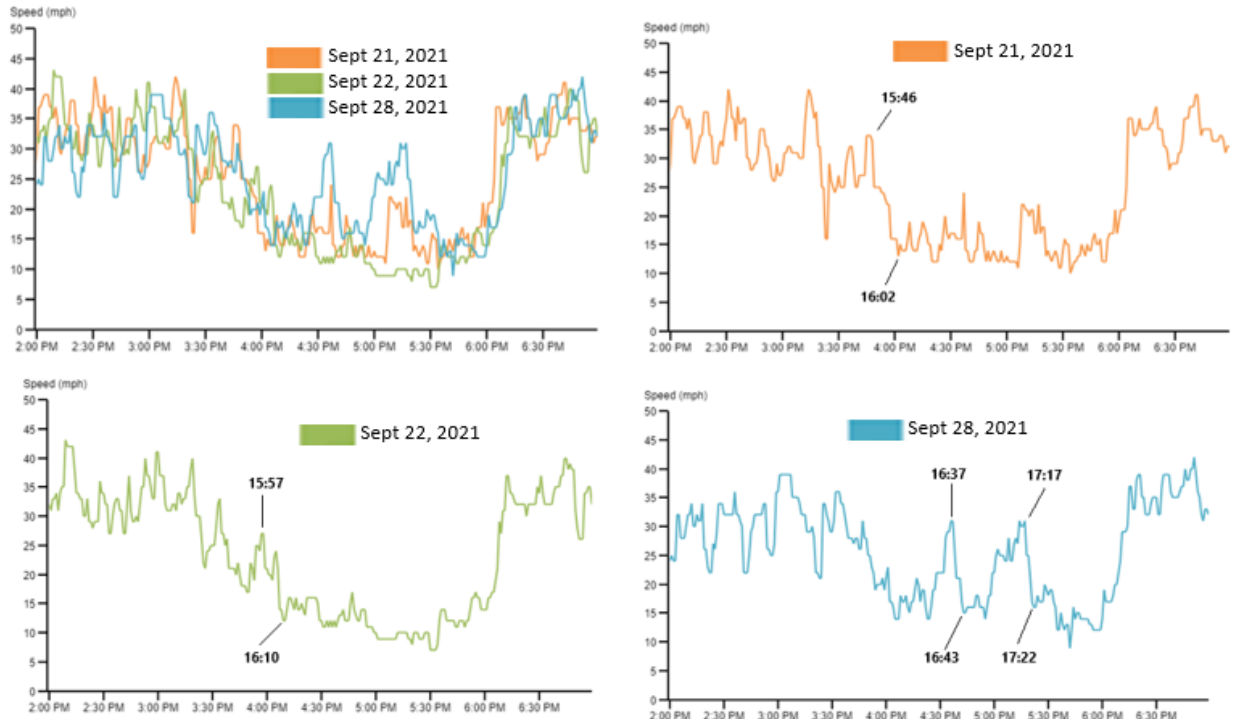


**Figure 14. INRIX speed profiles for the XD segment on IRR over the three days**

For September 28<sup>th</sup> data, cumulative plots were also created (see Figure 15) to show the variation in flow rates over time in the upstream and downstream of the XD segment. The vertical axis in this figure shows the normalized count where a background rate of 2,700 vehicles/hour is used. In other words, a horizontal line in this figure will correspond to a flow

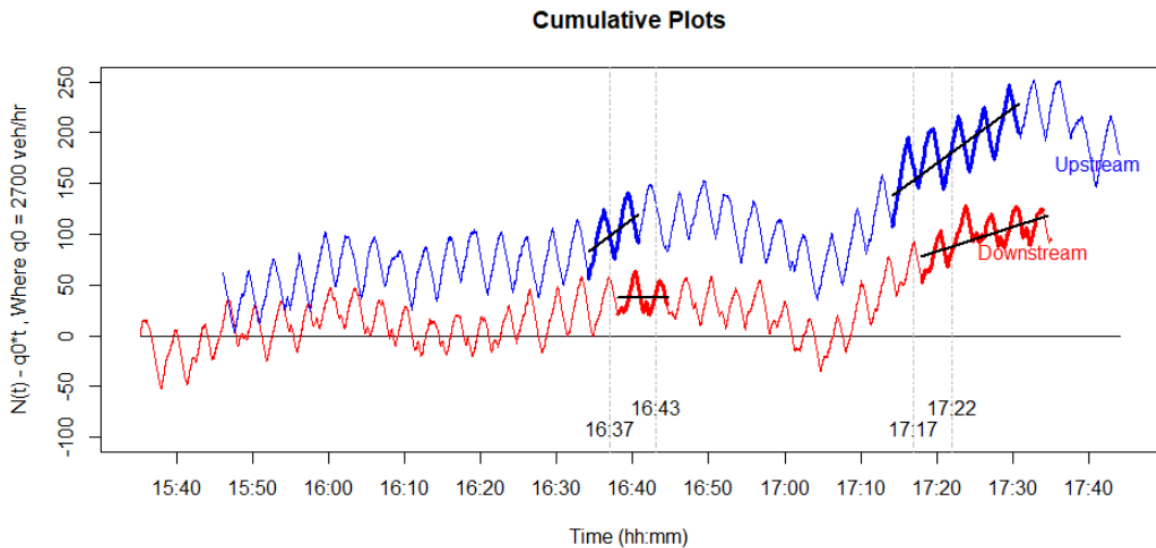


**Figure 15. Scaled cumulative count plots for the volumes at the upstream and downstream of the XD segment on IRR. At around 16:37 and 17:17 the INRIX speed values start dropping as shown in Figure 14.**

rate of 2,700 vehicles/hour. At approximately the critical times, the separation between upstream and downstream curves starts increasing. For example, at 16:37 PM, the arrival rate in the

upstream increases while the rate at the downstream starts diminishing. This leads to the accumulation of vehicles between upstream and downstream, and eventually the queue backs up to the upstream intersection. Similar observations can be made for the change in flow rates at 17:17 PM.

Table 5 and Table 6 show the parameters used in SW and VDF methods and the demand volumes estimated by these methods. For both methods, the estimated volumes are relatively close to the observed flow rates. The errors are less than 4%. These results demonstrate that the proposed methods are effective in estimating the demand volumes in oversaturated conditions.

**Table 5. Application of the SW method to the collected data on IRR**

Date	t <sub>1</sub>	t <sub>2</sub>	T (min)	U <sub>A</sub> (mph)	U <sub>C</sub> (mph)	w (mph)	q <sub>c</sub> (vph)	Est q <sub>A</sub> (vph)	Obs q <sub>A</sub> (vph)	%Err
9/21/2021	15:46	16:02	16	34	13	-1.24	2,736	2,892	2,936	-1.5%
9/22/2021	15:57	16:10	13	27	12	-1.53	2,565	2,737	2,741	-0.2%
9/28/2021	16:37	16:43	6	31	15	-3.31	2,754	3,037	3,069	-1.0%
9/28/2021	17:17	17:22	5	31	16	-3.97	3,114	3,446	3,348	2.9%

**Abbreviations used in the table:**

- Date - Date of data collection
- t<sub>1</sub> : The time when the oversaturation is estimated to begin based on the speed profiles
- t<sub>2</sub> : The estimated time at which the queue reaches the beginning of the XD segment
- T - t<sub>2</sub>-t<sub>1</sub> or the time it takes for the speed to drop from free flow speed to congested speed
- U<sub>A</sub> - Speed under free flow in mph (miles per hour)
- U<sub>C</sub> - Speed under congestion in mph (miles per hour)
- W - Speed of the Shock wave produced due to queuing under congestion in mph
- q<sub>c</sub> - Maximum flow (Capacity) across intersection observed in field in vph
- vph - Vehicles per hour
- Est q<sub>A</sub> - Estimated arrival rate of vehicles using Shock wave theory in vph
- Obs q<sub>A</sub> - Actual Observed arrival rate of vehicles in the field in vph
- % Err - Percentage error between the estimated and the actual arrival rates in the field

**Table 6. Application of the VDF method to the collected data on IRR**

Date	t1	t2	T min	I	k	U <sub>A</sub> mph	U <sub>C</sub> mph	Obs Delay (s)	c (vph)	x	d <sub>2</sub> (s)	Est q <sub>A</sub> (vph)	Obs q <sub>A</sub> (vph)	% Err
9/21/21	15:46	16:02	16	0.09	0.50	34	13	28.32	2,736	1.06	28.32	2,891	2,936	-1.5%
9/22/21	15:57	16:10	13	0.09	0.50	27	12	27.59	2,565	1.07	27.59	2,740	2,741	0.0%
9/28/21	16:37	16:43	6	0.09	0.50	31	15	20.51	2,754	1.11	20.51	3,059	3,069	-0.3%
9/28/21	17:17	17:22	5	0.09	0.50	31	16	18.02	3,114	1.12	18.02	3,478	3,348	3.9%

**Abbreviations used in the table:**

- Date - Date of data collection
- t<sub>1</sub> : The time when the oversaturation is estimated to begin based on the speed profiles
- t<sub>2</sub> : The estimated time at which the queue reaches the beginning of the XD segment
- T - t<sub>2</sub>-t<sub>1</sub> or the time it takes for the speed to drop from free flow speed to congested speed
- I - Upstream filtering/metering adjustment factor
- k - Incremental delay factor that is dependent on controller settings
- U<sub>A</sub> - Speed under free flow in mph (miles per hour)
- U<sub>C</sub> - Speed under congestion in mph (miles per hour)
- Obs Delay - Observed delay in seconds
- q<sub>C</sub> - Maximum flow (Capacity) across intersection observed in field in vph
- vph - Vehicles per hour
- X - Lane group v/c ratio or degree of saturation
- d<sub>2</sub> - Incremental delay
- Est q<sub>A</sub> - Estimated arrival rate of vehicles in vph
- Obs q<sub>A</sub> - Observed arrival rate of vehicles in vph
- % Err - Percentage error between the estimated and the actual arrival rates in the field

## DISCUSSION

Estimating DV for oversaturated conditions is nontrivial because of the difficulty in measuring flow rates when extensive queueing spans multiple segments and intersections. While the methods presented here appear promising, there are some important caveats to be noted.

- The proposed methods only capture the effects of vehicles arriving to the queue. In other words, the methods estimate the flow rate joining the back of the queue within the analysis period. The vehicles arriving to the back of the queue might be metered by potential upstream constrictions (e.g., other traffic signals). In such cases, the arrival rate to the back of the queue would be higher if there had been no constrictions in the upstream. Consequently, the estimated values could underestimate the true demand when the traffic flow in the upstream is metered.
- The proposed approach produces an estimated DV for the period  $T$ , not for the entire peak period. This period starts at the beginning of the oversaturation period and extends for a time  $T$ , depending on the length of the TMC/XD segment: the longer the segments, the longer the  $T$ . The demand volume rate beyond  $T$  is not estimated and may be higher or lower than the estimated values.
- Given the fluctuations in traffic volumes (see the field data in Table 5 and Table 6), it is important to produce estimates for multiple days and average the results to obtain more stable estimates.
- For extracting the critical times  $t_1$  and  $t_2$  from INRIX XD/TMC data, there is no automated method. The research team has attempted to develop an algorithm for this purpose, but the results have not been fully satisfactory. Therefore, these critical times are determined using manual inspection or a heuristic as explained in Appendix A.
- In this research, it was assumed that the corridor being studied is known to have oversaturation. No method is developed in this research to detect oversaturated conditions.
- To estimate demand volume, in addition to the TMC/XD speed data, the capacity or throughput of the congested segment is needed. This can be obtained from intersection turning movement counts which was the case for the IRR example presented in Table 5 and Table 6. If such data are not available, the capacity of the signalized intersection can be estimated based on signal timing and HCM methods. It should be noted that the SW method can be used for volume/capacity ratio estimation without the need for capacity data (see Equation 3).
- The presented methods are applicable to reasonably long segments (e.g., >500 meters), where vehicles could accumulate due to the constricted capacity. Short segments or corridors with numerous entry/exit points (e.g., in downtown areas) would result in complex flow dynamics and multiple origin-destination flows to be tracked. The presented methods are not applicable to such complex cases.

## CONCLUSIONS

- *Both HCM VDF-based and shockwave-based methods provide reasonably accurate estimates of the demand volume when tested with both the simulated data and the limited field data.* The estimated volumes from the models, when implemented on the field data, are within 4% of the observed volumes. For the simulated IRR corridor, the mean absolute percentage errors are 5.4% and 4.2% for the SW and VDF methods respectively.
- *INRIX speed data were shown to be a viable option for estimating demand or volume/capacity ratios for oversaturated corridors.* The INRIX XD data for the IRR corridor were used as the input for the two methods and were found to provide accurate estimates. The one-minute INRIX speed profiles give enough time resolution to capture the propagation of the queue across the XD/TMC segments. The critical times when the queue reaches the end or beginning of the segments can be identified effectively from INRIX data.
- *The methods perform better when the TMC/XD segments are longer than 500 m.* The simulation results show that the error rates drop significantly when the TMC/XD length is 500 meters or longer.
- *The proposed methods could be applied to corridors with multiple intersections, but additional steps are necessary to account for different entering flows.* As shown with the simulated data for the IRR corridor, when there are multiple entering flows, the methods produce an estimated demand volume corresponding to the net inflow to the main corridor (flows contributing to the queue). If the demand volumes coming from different sources need to be estimated, vehicle volumes need to be collected at the upstream points where the different flows (e.g., side street volumes) are entering the corridor.

## RECOMMENDATIONS

The overall results of this research suggest that the use of either the HCM VDF or the SW method for estimating v/c or demand volume for oversaturated conditions could be valuable, when applicable, for managers of planning-level studies. Additional field testing of the methods, discussed below in the Implementation section, could further confirm the benefits of using these methods. Managers of planning-level studies typically include, but are not limited to, TMPD, TED, and related District staff.

The reasons for not requiring that planning managers use the HCM VDF or the SW method estimating v/c or demand volume for oversaturated conditions in every case are threefold. First, these methods are applicable only if the volume is not directly observable through the appropriate placement of sensors. Second, while these methods have been shown to be feasible given the current types of data available in Virginia, they should not preclude other methods (e.g., those that rely on vehicle information) (Gao et al., 2019, 2020) should they become feasible in the future. Should other methods, with new types of data, enable smaller forecast to observed errors than those reported in this study (values ranged from 1.4% - 5.4%), such methods would also merit consideration. Third, for some planning level studies, it may be

the case that latent demand—e.g., the traffic that would use a particular corridor if it were not congested—is of greater interest than the demand volume that was the subject of this report. In that situation, the HCM VDF and SW methods may be informative but would require some additional analysis beyond the scope of this study’s findings in order to estimate latent demand.

If managers of planning level studies decide to use the HCM VDF or the SW method for estimating v/c or demand volume for oversaturated conditions in a corridor, three study recommendations are:

1. *The ODU research team, with assistance from VTRC as needed, should provide written guidance enabling readers who are not familiar with this report to implement the HCM VDF and SW methods.*
2. *The ODU research team, with assistance from VTRC as needed, should conduct a webinar for interested staff on how to use the HCM VDF and SW methods.*
3. *VTRC should conduct a pilot project implementing these methods for two corridors.*

## **IMPLEMENTATION AND BENEFITS**

### **Implementation**

Implementation of the recommendations will proceed in three phases.

#### *Phase 1. Immediate Term*

In support of recommendation 1, the ODU research team has provided instructions that enable reviewers after they have obtained an INRIX account, to perform the following steps: (1) download some (but not necessarily all) of data for Virginia corridors such as those that are the subject of this study (e.g., Route 29 in the Northern Virginia District [Figure 7] or Indian River Road in the Hampton Roads District [Figure 5]); (2) use the geometry of the intersection to identify candidate bottleneck locations; (3) compute the volume/capacity ratio due to the likely bottleneck location; (4) estimate capacity ( $q_c$ ) using the HCM or signal-based methods (even using an HCM lookup table), and then (5) estimate demand volume using the SW or VDF methods. These instructions, provided in Appendix A, were developed after the project panel had accepted the methods proposed herein.

This recommendation has already been implemented.

#### *Phase 2. Medium Term.*

The instructions in Appendix A will be conveyed in the form of a webinar conducted by the ODU research team and scheduled by the Virginia Transportation Research Council in consultation with ODU and planning partners. Invitees will include staff who are involved in planning-level studies, primarily those within the Transportation and Mobility Planning Division, the Traffic Engineering Division, and the district planning function, as well as other staff who

may have an interest in the role of oversaturated demand conditions for the purposes of project prioritization. Notably, the material to be presented in the webinar is not designed to enable attendees to obtain ground-truth data. Rather, this material will enable webinar attendees to apply the SW or VDF methods in situations currently faced by most VDOT analysts: a location is known to have congestion (but how much is not known), INRIX data are available, but ground truth data in the form of sensors or field observations are not available.

At this point, the instructions do not indicate that a particular amount of data (e.g., a week, month, or year) is needed, nor do they concern judgments such as possible seasonal variations in demand, or whether it is better to choose a week of average demand or a week of above-average demand. Such judgments are appropriate points of discussion for the webinar. At the conclusion of the webinar, attendees will be asked if they support (in terms of time) additional implementation work as discussed in Phase 3.

This webinar will be conducted prior to July 31, 2022.

### *Phase 3. Long Term.*

Phases 1 and 2 are being pursued as part of the original research, at no further cost to the Department. For Phase 3, VTRC implementation funds will be requested for a pilot project to be undertaken to deploy the tool at two corridors that involve real or potential transportation improvement investments. The pilot project may include up to four distinct elements, depending on the funds and staffing resources available. The scope of the pilot project will be established after the completion of the webinar in Phase 2 in order to move forward with the most productive elements.

The request for funding will occur prior to December 31, 2022.

- The pilot project may include the development of a macro-based tool that could automate the computation of  $T$  (based on  $t_1$  and  $t_2$ ) from INRIX data. This macro-based tool does not seek to replicate the judgment associated with picking a bottleneck location, but rather would help the analyst discern the transition from  $U_A$  to  $U_C$  and would help partially automate the SW and VDF methods.
- The pilot project may then indicate how future prioritization efforts, whether at the state or regional level, could make use of this newly available demand volume (or ratio of demand volume to capacity). As one example of a prioritization effort, the Commonwealth Transportation Board (2021) recently issued updated guidance on the calculation of benefits for evaluating candidate transportation investments. The SW or HCM VDF methods could be applied to two or more candidate transportation investments and the impact on project prioritization could be examined.
- If ATSPM data or field data become available, this pilot project could again entail a comparison with ground truth data; however, because of the large time cost associated with collecting field data or confirming the validity of sensor data, this third element requires careful consideration for inclusion in the pilot effort.

- The pilot effort may identify some short-term heuristics to address key limitations noted for these two approaches: they generally do not distinguish demand by lane group at an intersection, they are not appropriate for quantifying induced demand, and while they are applicable for arterial facilities, they are not suitable for ramps.

### **Benefits**

One benefit of implementing Recommendation 1 is to quickly determine the degree of oversaturation at bottleneck links. While more effort is required for estimating demand volume, the easier-to-estimate ratio of demand volume to capacity can be a useful screening tool, especially for situations such as IRR, where one can determine whether a potential bottleneck is impeding a relatively large or small demand (compared to its capacity). For example, page 61 of Commonwealth Transportation Board (2021) explicitly notes that “person throughput is only credited/scored if the facility is over capacity in the no-build project condition (has a volume to capacity ratio greater than 1.0).” Such language suggests that quick ways of estimating demand volume to capacity ratios for candidate transportation investments may be productive for entities that are considering candidate transportation investments that would be subject to that prioritization process.

A second benefit of comparing demand volumes as opposed to comparing observed volumes in congested situations is that demand volumes can differ regardless of the capacity of the roadway, where observed volumes can only differ up to the capacity of the roadway. The capacity of the roadway constrains the observed volumes and can mask the true demand. Further, when prioritizing projects based on their ability to reduce delay, one can weight these delays based on demand volume—which will differ from observed volume under oversaturated conditions.

As an illustration of this second benefit, consider how one would weight a project that would reduce delay if it were situated on IRR (the subject of Tables 5 and 6). Without this research, one would multiply the average vehicle delay reduction impacts by the observed volume (e.g.,  $q_c$  in Tables 5 and 6) which ranges from 2,565 vehicles/hour (on September 22, 2021) to 3,114 veh/hr (on September 28, 2021). With this research, one would likely use either the SW method (2,737-3,446 veh/hr) or the VDF method (e.g., 2,740-3,478 vehicles/hour). (Of course, one could also perform field data collection as well to get an exact value of 2,741-3,348 vehicles/hour, but such field validations are time consuming to perform and were one of the reasons for developing these other methods). If one chooses the average of the four days, one obtains the following volumes:

- Mean observed volume is 2,792
- Estimated demand volume (SW method) is 3,027 (8.4% higher than observed volume)
- Estimated demand volume (VDF method) is 3,042 (8.9% higher than observed volume)
- Perfect demand volume (field observation) is 3,023 (8.3% higher than observed volume)

Thus, the use of demand volume—without field observations—would yield a volume that is about 8.65% higher than observed volume—for a corridor similar to IRR. However, if one

instead used a corridor similar to the simulated two-lane facility with a signal, then the average of the 48 estimated demand volumes in Tables 1 and 2 (2,540) is about 27.45% higher than the observed volume (1,993). In short, demand volume will always be higher than observed volume (under congested conditions) but there may be variability in how much higher the demand volume is, depending on the location. The methods shown herein enable one to estimate the true demand volume—e.g., one evaluates investments based on the actual true demand for the capacity of the roadway rather than based on the existing built capacity of the roadway.

## ACKNOWLEDGMENTS

The contributions and feedback received from Peng Xiao, Marsha Fiol, Sanhita Lahiri, Amir Shahpar, and Chien-Lun Lan, who all served on the technical review panel, are highly appreciated. In addition, we are very grateful to John Miller who served as the project manager and helped the team schedule technical review panel meetings and access field data and provided invaluable comments and feedback to the team throughout the project. We are very grateful to Amy O’Leary and Mike Fitch from VTRC for providing invaluable comments that helped enhance the quality of the report. The team is also thankful to Shannon Warchol of Kimley-Horn for providing access to the ATSPM data. Graduate students Bishoy Kelleny and Ninad Parab from ODU helped with data collection and simulation modeling. Their help is also acknowledged.

## REFERENCES

- Akçelik, R., Travel time functions for transport planning purposes: Davidson's function, its time-dependent form and an alternative travel time function. *Australian Road Research*, Vol. 21, No.3, January 1991, pp. 49-59.
- Babinec, A., and Apeltauer J. On accuracy of position estimation from aerial imagery captured by low-flying UAVs. *International Journal of Transportation Science and Technology*, Vol. 5, No. 3, October 2016, pp. 152-166.
- Ban, X., Hao, P., and Sun, Z. Real time queue length estimation for signalized intersections using travel times from mobile sensors. *Transportation Research Part C: Emerging Technologies*, Vol. 19, No. 6, December 2011, pp. 1133-1156.
- Barmounakis, E., and Geroliminis, N. On the new era of urban traffic monitoring with massive drone data: The pNEUMA large-scale field experiment. *Transportation Research Part C Emerging Technologies*, Vol. 111, February 2020, pp. 50-71.
- Barmounakis, E., Vlahogianni, E., and Golias, J. Unmanned Aerial Aircraft Systems for transportation engineering: Current practice and future challenges. *International Journal of Transportation Science and Technology*, Vol. 5, No. 3, October 2016, pp. 111-122.
- Berry, D.S., Volume Counting for Computing Delay at Signalized Intersections. *ITE Journal*, Vol. 57, No. 3, March 1987, pp. 21-23.

- Cetin, M. and Anuar, K.A. Using probe vehicle trajectories in stop-and-go waves for inferring unobserved vehicles. 5th IEEE International Conference on Models and Technologies for Intelligent Transportation Systems (MT-ITS), 2017, pp.333-338.
- Cetin, M., Estimating Queue Dynamics at Signalized Intersections from Probe Vehicle Data: Methodology Based on Kinematic Wave Model. *Transportation Research Record*, Vol. 2315, No.1, January 2012, pp. 164-172.
- Cetin, M., Foytik, P., Son, S., Khattak, A.J, Robinson, R.M., and Lee, J. Calibration of Volume-Delay Functions for Traffic Assignment in Travel Demand Models, Transportation Research Board 91st Annual Meeting, Washington DC, United States, 2012.
- Cheng, Y., Qin, X., Jin, J., Ran, B., and Anderson, J. Cycle-by-Cycle Queue Length Estimation for Signalized Intersections Using Sampled Trajectory Data. *Transportation Research Record*, Vol. 2257, No. 1, January 2011, pp. 87-94.
- Cho, H-J., and Tseng, M-T. Shockwave Detection for Electronic Vehicle Detectors. Computational Science – ICCS 2007, Lecture Notes in Computer Science, Vol. 4490. Springer, Berlin, Heidelberg, 2007, pp. 275-282.
- Cho, H-J., Tseng, M-T., and Hwang, M-C. Using detection of vehicular presence to estimate shockwave speed and upstream traffics for a signalized intersection. *Applied Mathematics and Computation*, Vol. 232, No. 1, April 2014, pp. 1151-1165.
- Coifman, B., Beymer, D., McLauchlan, P., and Malik, J. A real-time computer vision system for vehicle tracking and traffic surveillance. *Transportation Research Part C: Emerging Technologies*, Vol. 6, No. 4, August 1998, pp. 271-288.
- Comert, G., and Cetin, M. Queue length estimation from probe vehicle location and the impacts of sample size. *European Journal of Operational Research*, Vol. 197, No. 1, August 2009, pp. 196-202.
- Commonwealth Transportation Board. SMART SCALE Technical Guide. Richmond, Virginia 2021e. <https://smartscale.org/documents/2020documents/technical-guide-2022.pdf>. Accessed October 4, 2021.
- Davidson, K.B. A flow travel time relationship for use in transportation planning. 3rd Australian Road Research Board (ARRB) Conference, Sydney, Vol. 3, No. 1, 1966, pp.183-194.
- Feng, R., Fan, C., Li, Z., and Chen, X. Mixed Road User Trajectory Extraction from Moving Aerial Videos Based on Convolution Neural Network Detection. *IEEE Access*, Vol. 8, March 2020, pp. 43508-43519.
- Foytik, P., Cetin, M., and Robinson, R.M. Calibration of BPR Function Based on Link Counts

- and Its Sensitivity to Varying Demand. Transportation Research Board 92nd Annual Meeting, Washington DC, United States, 2013.
- Gao, K., Han, F., Dong, P., Xiong, N., and Du, R. Connected Vehicle as a Mobile Sensor for Real Time Queue Length at Signalized Intersections. *Sensors*, Vol. 19, No.9, May 2019, Web Journal Access: <https://www.mdpi.com/1424-8220/19/9/2059>, Accessed, April 15, 2021.
- Gao, K., Huang, S., Han, F., Li, S., Wu, W., and Du, R. An Integrated Algorithm for Intersection Queue Length Estimation Based on IoT in a Mixed Traffic Scenario. *Applied Science*, Vol. 10, No. 6, 2020, Web Journal Access: <https://www.mdpi.com/2076-3417/10/6/2078>, Accessed April 15, 2021.
- Hao, P., Sun, Z., Ban, X., Guo, D., and Ji, Q. Vehicle index estimation for signalized intersections using sample travel times. *Transportation Research Part C: Emerging Technologies*, Vol. 36, November 2013, pp. 513-529.
- Huntsinger, L.F. and Roupail, N.M. Bottleneck and Queuing Analysis: Calibrating Volume–Delay Functions of Travel Demand Models. *Transportation Research Record*, Vol. 2255, No. 1, January 2011, pp. 117-124.
- Islam, M.K., *Real-Time Queue Length Estimation Using Probe Vehicles with Cumulative Input-Output Technique*. University of Calgary, Calgary, AB, 2013.
- Jian, L., Li, Z., Yang, X., Wu, W., Ahmad, A., and Jeon, G. Combining Unmanned Aerial Vehicles With Artificial-Intelligence Technology for Traffic-Congestion Recognition: Electronic Eyes in the Skies to Spot Clogged Roads. *IEEE Consumer Electronics Magazine*, Vol. 8, No. 3, May 2019, pp. 81-86.
- Ke, R., Feng, S., Cui, Z., and Wang Y. Advanced Framework for Microscopic and Lane-level Macroscopic Traffic Parameters Estimation from UAV Video. *IET Intelligent Transport Systems*, Vol. 14, No. 4, April 2020, pp. 724-734.
- Khan, M. A., Ectors, W., Bellemans, T., Janssens, D., and Wets, G. Unmanned Aerial Vehicle-Based Traffic Analysis: A Case Study for Shockwave Identification and Flow Parameters Estimation at Signalized Intersections. *Remote Sensing*, Vol. 10, No. 3, 458, March 2018, Web Journal Access: <https://www.mdpi.com/2072-4292/10/3/458>, Accessed April 2, 2020.
- Khan, M. A., Ectors, W., Bellemans, T., Janssens, D., and Wets, G. UAV-Based Traffic Analysis: A Universal Guiding Framework Based on Literature Survey. *Transportation Research Procedia*, Vol. 22, 2017a, pp. 541-550.
- Khan, M. A., Ectors, W., Bellemans, T., Janssens, D., and Wets, G. Unmanned Aerial Vehicle-Based Traffic Analysis: Methodological Framework for Automated Multivehicle Trajectory Extraction. *Transportation Research Record*, Vol. 2626, No. 1, January 2017b, pp. 25-33.

- Khan, N. A., Jhanjhi, N.Z., Brohi, S.N., Usmani, R.S.A., and Nayyar, A. Smart traffic monitoring system using Unmanned Aerial Vehicles (UAVs). *Computer Communications*, Vol.157, No. 1, May 2020, pp. 434-443.
- Kim, E-J., Park, H-C, Ham, S-W., Kho, S-Y., and Kim, D-K. Extracting Vehicle Trajectories Using Unmanned Aerial Vehicles in Congested Traffic Conditions. *Journal of Advanced Transportation*, Vol. 2019, Article ID 9060797, April 2019, Web Journal Access: <https://www.hindawi.com/journals/jat/2019/9060797/> Accessed April 10, 2020.
- Kucharski, R. and Drabicki, A. Estimating Macroscopic Volume Delay Functions with the Traffic Density Derived from Measured Speeds and Flows. *Journal of Advanced Transportation*, Vol. 2017, Article ID 4629792, February 2017. Web Journal Access: <https://www.hindawi.com/journals/jat/2017/4629792/>, Accessed March 25, 2020.
- Li, F., Tang, K., Yao J., and Li, K. Real-Time Queue Length Estimation for Signalized Intersections Using Vehicle Trajectory Data. *Transportation Research Record*, Vol. 2623, No. 1, January 2017, pp. 49-59.
- Li, H., Chen, N., Qin, L., Jia, L., and Rong, J. Queue length estimation at signalized intersections based on magnetic sensors by different layout strategies. *Transportation Research Procedia*, Vol. 25, 2017, pp. 1626-1644.
- Li, X., Wu, Y-J., and Chiu, Y-C. Volume Estimation using Traffic Signal Event-Based Data from Video-Based Sensors. *Transportation Research Record*, Vol. 2673, No. 6, April 2019, pp. 22-32.
- Liu, H., Wu, X., Ma, W., and Hu, H. Real-time queue length estimation for congested signalized intersections. *Transportation Research Part C: Emerging Technologies*, Vol.17, No. 4, August 2009, pp. 412-427.
- Luo, X., Liu, B., Jin, P.J., Cao, Y., and Hu, W. Arterial Traffic Flow Estimation Based on Vehicle-to-Cloud Vehicle Trajectory Data Considering Multi-Intersection Interaction and Coordination. *Transportation Research Record*, Vol 2673, No. 6, April 2019, pp. 68-83.
- Luo, X., Ma, D., Jin, S., Gong, Y., and Wang, D. Queue Length Estimation for Signalized Intersections Using License Plate Recognition Data. *IEEE Intelligent Transportation Systems Magazine*, Vol. 11, No. 3, Fall 2019, pp. 209-220.
- Ma, D., Luo, X., Jin, S., Guo, W., and Wang, D. Estimating Maximum Queue Length for Traffic Lane Groups Using Travel Times from Video-Imaging Data. *IEEE Intelligent Transportation Systems Magazine*, Vol. 10, No. 3, Fall 2018, pp. 123-134.
- Ma, D., Luo, X., Li, W., Jin, S., Guo, W., and Wang, D. Traffic demand estimation for lane groups at signal-controlled intersections using travel times from video-imaging detectors. *IET Intelligent Transport Systems*, Vol, 11, no. 4, May 2015, pp. 222-229.

- Ma, W. and Qian, S. High-Resolution Traffic Sensing with Autonomous Vehicles. Pre-Print Edition, *Electrical Engineering and Systems Science, Signal Processing*, arXiv:1910.02376v1 [eess.SP], Oct 2019. Web Access: [https://www.researchgate.net/publication/336288358\\_High-Resolution\\_Traffic\\_Sensing\\_with\\_Autonomous\\_Vehicles](https://www.researchgate.net/publication/336288358_High-Resolution_Traffic_Sensing_with_Autonomous_Vehicles) Accessed April 10, 2020.
- Morgul, E., Yang, H., Kurkcu, A., Ozbay, K., Bartin, B., Kamga, C., and Salloum, R. Virtual Sensors: Web-Based Real-Time Data Collection Methodology for Transportation Operation Performance Analysis. *Transportation Research Record*, Vol. 2442, No. 1, January 2014, pp. 106-116.
- Moses, R., Mtoi, E., and Ruegg, S. *Development of Speed Models for Improving Travel Forecasting and Highway Performance Evaluation*. BDK-83-977-14. Florida Department of Transportation, Tallahassee, FL, December 2013.
- Mtoi, E. and Moses, R. Calibration and Evaluation of Link Congestion Functions: Applying Intrinsic Sensitivity of Link Speed as a Practical Consideration to Heterogeneous Facility Types Within Urban Network. *Journal of Transportation Technologies*, Vol. 4, No. 2, April 2014, pp. 141-149.
- Mück, J., Using detectors near the stop-line to estimate traffic flows. *Traffic Engineering and Control*, Vol. 43, No. 11, December 2002, pp. 429-434.
- Papageorgiou, M. and Varaiya, P. Link Vehicle-Count—the Missing Measurement for Traffic Control. *IFAC Proceedings Volumes*, Vol. 42, No. 15, 2009, pp. 224-229.
- Ramezani, M. and Geroliminis, N. Exploiting probe data to estimate the queue profile in urban networks. 16th International IEEE Conference on Intelligent Transportation Systems (ITSC 2013), 2013, pp. 1817-1822.
- Ramezani, M. and Geroliminis, N. Queue Profile Estimation in Congested Urban Networks with Probe Data. *Computer-Aided Civil and Infrastructure Engineering*, Vol. 30, No. 6, June 2015, pp. 414-432.
- Regional Integrated Transportation Information System (RITIS). <https://ritis.org/intro>. Accessed November 12, 2021.
- Salahshour, B., Nezafat, R.V., and Cetin, M. Estimation of Unobserved Vehicles in Congested Traffic from Probe Vehicle Samples, International Conference on Transportation and Development 2019, August 2019, pp. 24-35.
- Shahrbabaki, R.M., Safavi, A.A., Papageorgiou, M., and Papamichail, I. A data fusion approach for real-time traffic state estimation in urban signalized links. *Transportation Research Part C: Emerging Technologies*, Vol. 92, July 2018, pp. 525-548.
- So, J., Stevanovic, A., and Ostojic, M. Methodology to Estimate Volume& Capacity Ratios at

- Traffic Signals Based on Upstream-Link Travel Times. *Journal of Transportation Engineering, Part A: Systems*, Vol. 143, No. 4, April 2017, Article ID 04017002, Web Journal Access: <https://ascelibrary.org/doi/full/10.1061/JTEPBS.0000021>, Accessed April 2, 2020.
- Tan, C., Yao, J., Tang, K., and Sun, J. Cycle-Based Queue Length Estimation for Signalized Intersections Using Sparse Vehicle Trajectory Data. *IEEE Transactions on Intelligent Transportation Systems*, Vol. 22, No. 1, January 2021, pp. 91-106.
- Taylor, M.A.P. Parameter Estimation and Sensitivity of Parameter Values in a Flow-Rate/Travel-Time Relation. *Transportation Science*, Vol. 11, No. 3, August 1977, pp. 275-292.
- Transportation Research Board (TRB), *Highway Capacity Manual (HCM2000)*, Transportation Research Board, USA., 2000.
- Wang, L. *Design, Data Collection, and Driver Behavior Simulation for the Open-Mode Integrated Transportation System (OMITS)*, Civil Engineering and Engineering Mechanics, Columbia University, 2016.
- Wu, X., Liu, H., and Gettman, D. Identification of oversaturated intersections using high-resolution traffic signal data. *Transportation Research Part C: Emerging Technologies*, Vol. 18, No. 4, August 2010, pp.626-638.
- Yahia, C.N., Scott, S.E., Boyles, S.D., Claudel, C.G. Unmanned Aerial Vehicle Path Planning for Traffic Estimation and Detection of Non-Recurrent Congestion, Transportation Research Board 98th Annual Meeting, Washington DC, United States, 2019.
- Yang, H., Ozbay, K., and Xie, K. Improved Travel Time Estimation for Reliable Performance Measure Development for Closed Highways. *Transportation Research Record*, Vol. 2526, No. 1, January 2015, pp. 29-38.
- Yao, J. and Tang, K. Cycle-based queue length estimation considering spillover conditions based on low-resolution point detector data. *Transportation Research Part C: Emerging Technologies*, Vol. 109, December 2019, pp. 1-18.
- Zhang, H., Liu, H.X., Chen, P., Yu, G., and Wang, Y. Cycle-Based End of Queue Estimation at Signalized Intersections Using Low-Penetration-Rate Vehicle Trajectories. *IEEE Transactions on Intelligent Transportation Systems*, Vol. 21, No. 8, August 2019, pp. 3257-3272.
- Zhang, Z., Liu, H., Rai, L., and Zhang, S. Vehicle Trajectory Prediction Method Based on License Plate Information Obtained from Video-Imaging Detectors in Urban Road Environment. *Sensors*, Vol. 20, No. 5, 1258, February 2020, Web Journal Access: <https://doi.org/10.3390/s20051258>, Accessed April 1, 2020.

- Zhao, Y., Zheng, J., Wong, W., Wang, X., Meng, Y., and Liu, H.X. Various methods for queue length and traffic volume estimation using probe vehicle trajectories. *Transportation Research Part C: Emerging Technologies*, Vol. 107, October 2019, pp. 70-91.
- Zheng, J. and Liu, H.X. Estimating traffic volumes for signalized intersections using connected vehicle data. *Transportation Research Part C: Emerging Technologies*, Vol. 79, June 2017, pp. 347-362.
- Zheng, J., *Data-Driven Applications for Connected Vehicle Based Traffic Signal Systems*, University of Michigan, 2016.
- Zhu, J., Sun, K., Jia, S., Li, Q., Hou, X., Lin, W., Liu, B., and Qiu, G. Urban Traffic Density Estimation Based on Ultrahigh-Resolution UAV Video and Deep Neural Network. *IEEE Journal of Selected Topics in Applied Earth Observations and Remote Sensing*, 2018. Vol. 11, no. 12, December 2018, pp. 4968-4981.

## APPENDIX A: STEPS IN APPLYING THE SW AND VDF METHODS

This section explains the steps taken in applying the SW and HCM VDF methods. Overall, the following three main steps need to be completed in applying the methods.

- Step 1: Identifying an XD or TMC segment along the oversaturated corridor for the analysis
- Step 2: Extracting key parameters from the XD or TMC speed profiles
- Step 3: Applying the SW and HCM VDF methods

These steps are explained in detail below by using data from a sample congested corridor in Virginia Beach, VA. The IRR eastbound corridor is selected as an illustrative example since the team collected field data from this site as discussed in the report.

### Step 1: Identifying an XD or TMC Segment Along the Oversaturated Corridor

For a given oversaturated corridor, there may be multiple potential XD or TMC segments affected by traffic congestion. These segments typically have varying lengths, different road geometry, access points, and speed profiles. As indicated in the report, segments shorter than 500 meters do not provide enough range to apply the methods effectively. In addition, presence of significant access points with heavy turning volumes requires additional work to track entry and exit of volumes from/to the segment. Such access points may introduce additional noise to the INRIX speed data, making it difficult to analyze the speed for the main through movement across the segment. Therefore, before applying the method, the potential XD or TMC segments should be carefully analyzed. In other words, one should not expect that the proposed methods would yield accurate results for any oversaturated segment. The proposed methods are based on established traffic flow principles and should produce accurate results if the underlying assumptions are valid. The assumptions are more likely to be valid for segments that have reasonable lengths and minimal amount of traffic turbulence and disruptions.

As shown in the report, the proposed methods rely on two critical time stamps ( $t_1$  and  $t_2$ ) to be extracted from the speed profiles. The first parameter,  $t_1$ , marks the start of the oversaturation period for the segment being analyzed, whereas  $t_2$  the time when the queue reaches the beginning of the XD or TMC segment. How  $t_1$  and  $t_2$  are extracted from speed profiles is explained in the next subsection. However, before that, the selected XD or TMC segments should have speed profiles amenable for this purpose. While the team did not develop a precise test or technique to check whether an XD segment is suitable for the purpose, the following guidance is provided:

“The speed profiles (over multiple days) should exhibit a consistent pattern with a significant drop in speeds (e.g., from 40 mph to 20 mph) that takes place within a ‘meaningful’ period  $T$  ( $T = t_2 - t_1$ ). In addition, after  $t_2$ , the speed values should stay somewhat stable (at  $U_C$ ) for a reasonable duration (e.g., more than 5 minutes).”

There is a direct relationship between the volume/capacity ratio (i.e., degree of saturation) and  $T$  (duration of speed transition from  $u_A$  to  $u_C$ ). Figure A1, constructed based on Equation 3, shows the relationship between  $T$  and volume/capacity ratio for a hypothetical

segment where speed before oversaturation starts ( $u_A$ ) is assumed to be 40 mph and the speed within the queue ( $u_C$ ) 20 mph (assuming  $u_C$  is about half of  $u_A$  is reasonable based on profiles presented earlier in the report in Figure 1 and Figure 14). For example, if the XD segment is 0.5 mi long, and volume/capacity ratio is 1.05, then T is expected to be 14 minutes. In this example, if the observed T values from speed profiles are much larger than 14 minutes (e.g., 60 minutes), this would indicate that there is no significant oversaturation to be estimated/measured and, hence, applying the proposed methods here would not be plausible. If T is too long for the given segment length, it will imply that the corridor is lightly oversaturated, or the demand volume is at or close to capacity. As volume/capacity ratio approaches 1.0, T gets larger very quickly and approaches to infinity. Producing accurate predictions for relatively low volume/capacity ratios (e.g., between 1.0 and 1.05), therefore, will be difficult. To avoid making predictions for inherently a challenging range, one can set a criterion for a lower bound of volume/capacity ratio. For example, if this lower bound is selected to be 1.05, this implies that T should not be larger than 14 for 0.5 mi segments in the hypothetical case in Figure A1. Therefore, the applicability of the methods should be limited to speed profiles that meet these criteria.

The second sentence in the above guidance is about for how long the speed values remain approximately stable at around  $u_C$ . As explained in Methods section, the queue under oversaturation eventually reaches the beginning of the TMC/XD segment (since its length is finite). As long as the queue (or congestion) spans the entire length of the TMC segment, and the downstream conditions remain stable, the probe vehicle speeds will remain approximately constant. Therefore, this condition is expected to persist for a noticeable duration. On the other hand, if the speed drops to  $u_C$  but very quick goes back to a higher value (e.g., within 1 or 2 minutes), this may be due to temporary events like incidents, and unlikely to be due to oversaturation.

To show an example, INRIX data for the IRR eastbound corridor were selected as an illustrative example. Figure A2 shows three distinct XD segments along this corridor. XD1 is the same segment that was analyzed before in the Results section. The intersection of Kempsville Road and Indian River Rd is the major bottleneck. XD2 is in the upstream of this bottleneck and is relatively short (~1000 ft). Speed profiles for three segments are shown in Figures A3 through A5. These are produced from the RITIS system by using the Performance Charts option within the Probe Data Analytics Tools. The selected speeds correspond to September 2021 weekday data and the aggregation interval is set to one minute. As it can be observed in Figure A5, there is no congestion on XD3 since this segment is at the downstream of the bottleneck. XD2 is immediately in the upstream of the bottleneck, however, it does not show a noticeable drop in speed in a relatively short period of time. On the other hand, the speed profile for XD1 in Figure A3 meets the guidance described above. The speed is dropping to a low value of approximately 15 mph at around 4:00 PM and staying stable at the low value for almost 2 hours. Therefore, for this corridor XD1 should be selected for the analysis and for the application of the proposed methods.

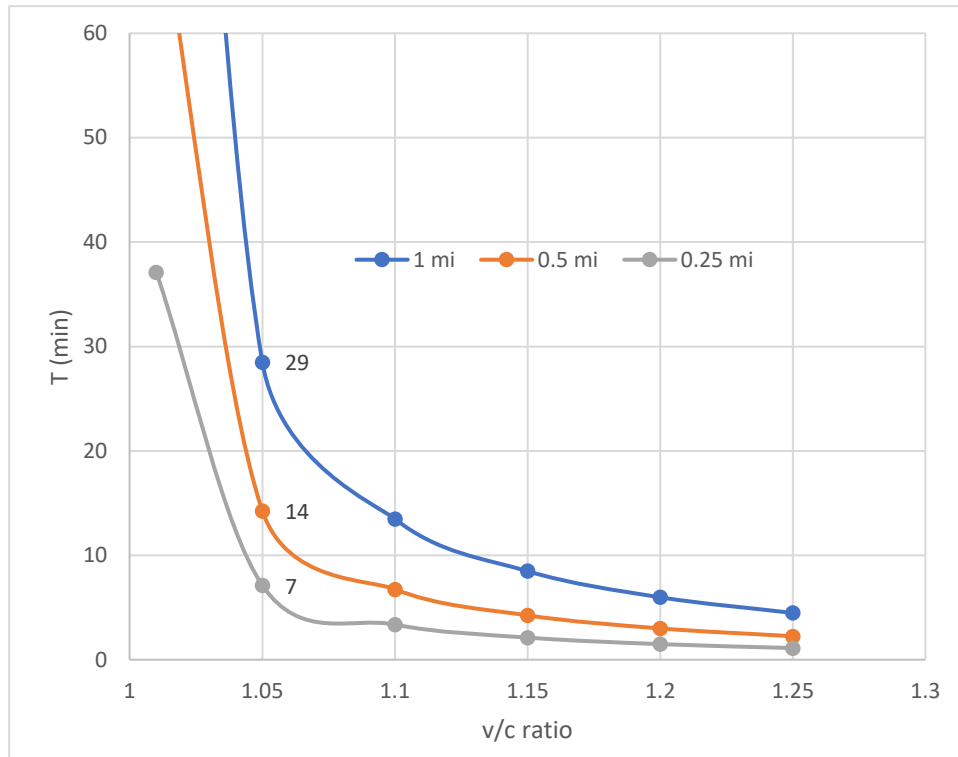


**Figure A1.** The relationship between T (duration of speed transition) and v/c ratio for a hypothetical case where speed before oversaturation starts is assumed to be 40 mph and the speed within the queue 20 mph. The three lines correspond to three different XD or TMC segment lengths (0.25 mi, 0.50 mi, and 1.00 mi).

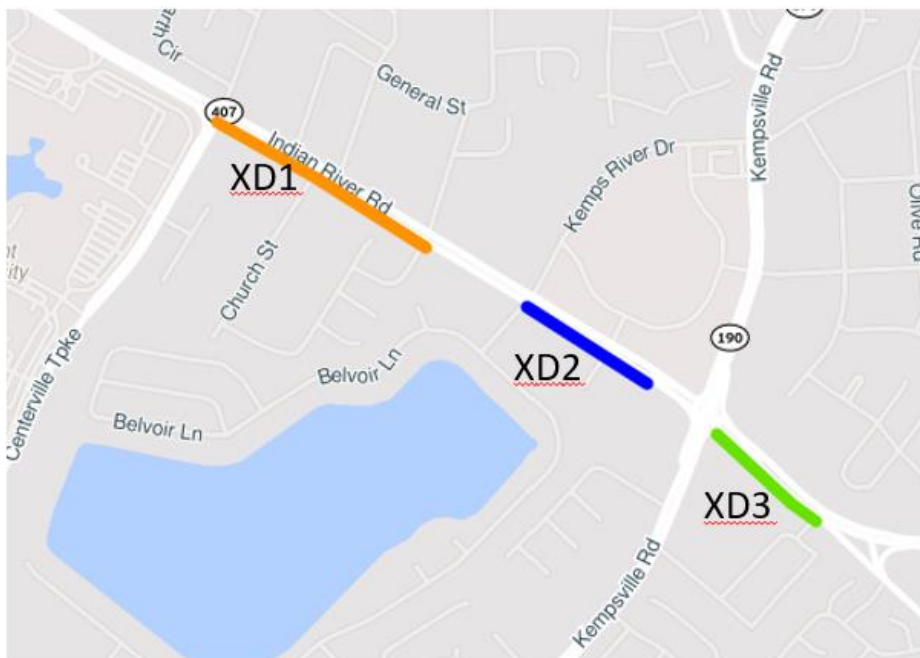


**Figure A2.** Three INRIX XD segments along Indian River Rd EB

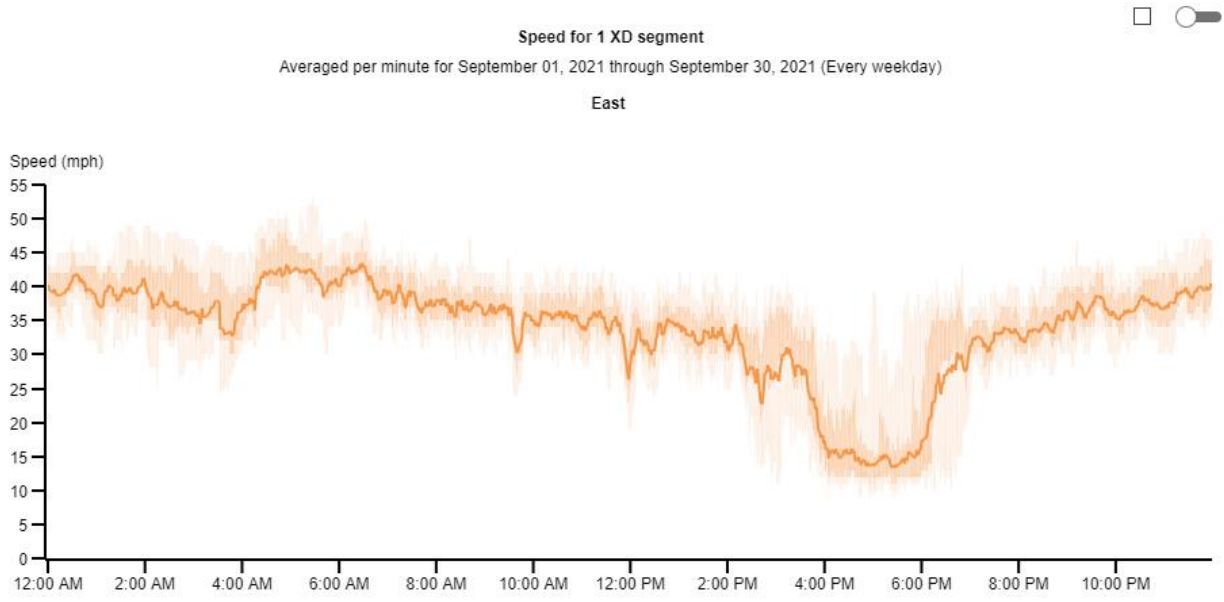


**Figure A3. Speed profile for XD1 segment shown in Figure A2**

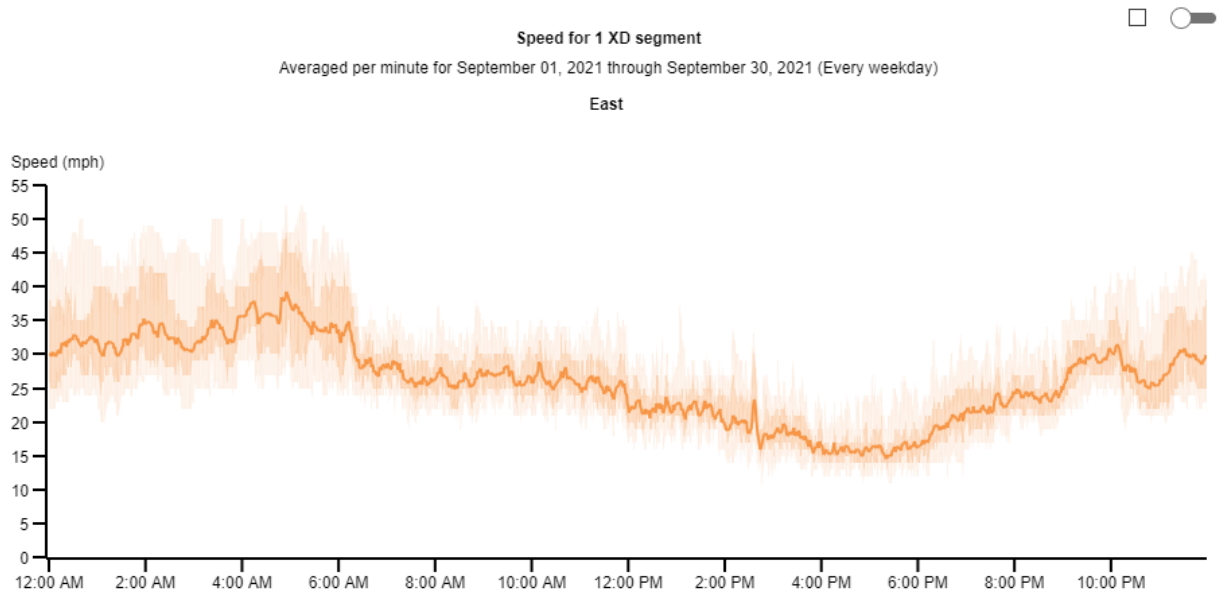


**Figure A4. Speed profile for XD2 segment shown in Figure A2**



**Figure A5. Speed profile for XD3 segment shown in Figure A2**

**Step 2: Extracting key parameters from the XD or TMC speed profiles**

Once a suitable XD or TMC segment is identified, the next step is to extract the key information from the speed profiles. These include  $t_1$  and  $t_2$  and the speed values  $u_A$  and  $u_C$ . The following heuristic is employed to determine these parameters.

First, the approximate period to locate the critical times is identified based on a visual inspection of the average speed profiles in Figure A3. Based on this figure, the speeds are dropping around 4:00 PM. Therefore, the critical times should be searched around 4 PM on the speed profiles for an individual day. The speed profile for September 21<sup>st</sup>, 2021, is shown in Figure A6 as an example. On this day, there is a clear drop in the speed at around 4:00 PM; the speed is dropping to around 15 mph and remaining at that low level for a considerable duration. To locate  $t_2$  the profile is followed from high speed towards low speeds. After reaching 13 mph at 4:02 PM, the speed values start fluctuating up and down. Therefore,  $t_2$  is set to 4:02 PM. Going back in time from 4:02 PM, speed values keep increasing until 3:46 PM is reached and subsequently start fluctuating. Therefore,  $t_1$  is set to 3:46 PM.

Once  $t_1$  and  $t_2$  are determined, the speed values  $u_A$  and  $u_C$  are simply found by reading the speeds from the chart corresponding to these time stamps. If the analyst does not want to download the INRIX data to a local computer for processing, the Performance Charts within the Probe Data Analytics Tools can be utilized to read off these values. The speed values are displayed by hovering the mouse over the chart and clicking on the value at a given time stamp. For this example, the speed values are 34 mph and 13 mph respectively for  $u_A$  and  $u_C$ .

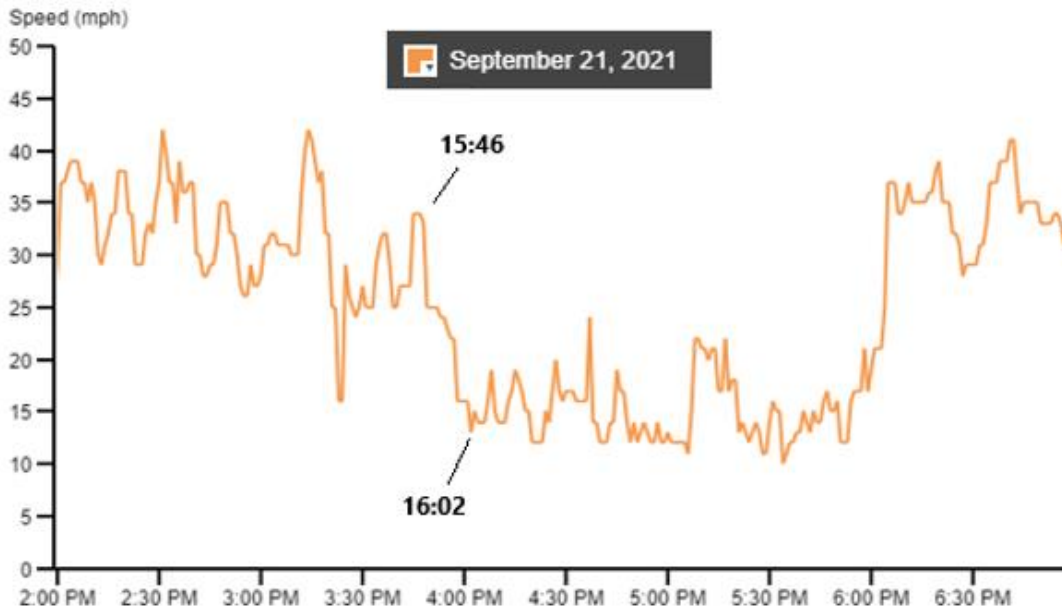


Figure A6. Speed profile for XD1 segment shown in Figure A2

### Step 3: Applying the SW and HCM VDF methods

Application of the SW method involves substituting the known parameters into the equations presented earlier. To illustrate it, the method is applied to the data extracted from Figure A6. The following parameters were extracted:

- $t_1 = 15:46$
- $t_2 = 16:02$
- $U_A = 34 \text{ mph}$
- $U_C = 13 \text{ mph}$

Therefore, the duration of speed transition from  $u_A$  to  $u_c$  is:

$$T = 16:02 - 15:46 = 16 \text{ minutes}$$

Since the XD segment length is 0.33 mi, the SW speed  $w$  is then as follows.

$$w = 0.33 / (16/60) = 1.24 \text{ mph.}$$

The ratio of volume/capacity or  $v/c$  can be found from Equation 3 as 1.06.

$$\frac{v}{c} = \frac{q_A}{q_c} = \frac{1 - \frac{w}{u_c}}{1 - \frac{w}{u_A}} = \frac{1 + 1.24/13}{1 + 1.24/34} = 1.06$$

Figure A6 does not indicate the discharge flow rate  $q_c$ . However, field data were collected at this site to measure  $q_c$ . According to the observations,  $q_c$  is 2,736 vph. The estimated demand volume can be found by entering the known parameters in Equation 4.

$$q_A = \frac{q_c - w \frac{q_c}{u_c}}{1 - \frac{w}{u_A}} = \frac{2736 + 1.24 \frac{2736}{13}}{1 + \frac{2736}{34}} = 2,892 \text{ vph}$$

Note that in applying Equations 3 and 4, the shock wave is moving backwards. Thus,  $w$  is a negative number such that its subtraction is shown as adding a positive number (right side of each equation).

Similarly, the application of the HCM VDF method involves entering the known quantities into the VDF equation:

$$d_2 = 900 T \left[ (X - 1) + \sqrt{(X - 1)^2 + \frac{8kIX}{cT}} \right]$$

This equation needs to be solved for the degree of saturation  $X$  (i.e.,  $v/c$  ratio) for the measured average delay  $d_2$ . For the same example, the delay  $d_2$  is computed as:

$$d_2 = \frac{\frac{L}{u_c} - \frac{L}{u_A}}{2} * 3600 = \frac{\frac{0.33}{13} - \frac{0.33}{34}}{2} * 3600 = 28.32 \text{ sec}$$

The remaining terms in Equation (4) include  $T$ ,  $k$ ,  $I$ , and  $c$ .  $T$  is the analysis period and taken to be  $t_2 - t_1$ . The parameters  $k$  and  $I$  are looked up from the HCM tables (Exhibit 16-13 for  $k$  values and Exhibit 15-9 for  $I$  in HCM 2000). The capacity  $c$  is the intersection approach throughput and is 2,736 vph in this example. Using the known inputs, the VDF equation is written as:

$$28.32 = 900(16/60) \left[ (X - 1) + \sqrt{(X - 1)^2 + \frac{8(0.5)(0.09)X}{(2736)(16/60)}} \right]$$

With these inputs, the best  $X$  value satisfying this equation can be found by using the Solver function in MS Excel. For this case,  $X = 1.06$ . Multiplying 1.06 by  $c$  gives the estimated demand volume of 2,891 vph.



**APPENDIX B: TRAFFIC COUNTS**

**Upstream Volume Counts at the Indian River Road Corridor**

<u>9/21/2021</u>		<u>9/22/2021</u>		<u>9/28/2021</u>	
<b>Time flow ended</b>	<b>Count</b>	<b>Time flow ended</b>	<b>Count</b>	<b>Time flow ended</b>	<b>Count</b>
15:22:51	149	15:42:59	153	15:50:50	160
15:26:16	145	15:46:18	147	15:54:10	164
15:29:34	144	15:49:35	138	15:57:30	151
15:32:53	151	15:52:59	147	16:00:50	172
15:36:13	148	15:56:17	158	16:04:10	141
15:39:38	162	15:59:33	142	16:07:30	157
15:42:55	171	16:02:52	164	16:10:50	143
15:46:19	156	16:06:12	170	16:14:10	156
15:49:36	146	16:09:40	159	16:17:30	169
15:52:57	171	16:12:58	166	16:20:50	150
15:56:18	163	16:16:18	157	16:24:10	158
15:59:39	166	16:19:30	153	16:27:30	150
16:02:58	156	16:23:01	161	16:30:50	161
16:06:19	140	16:26:18	150	16:34:10	158
16:09:43	152	16:29:37	154	16:37:30	183
16:12:58	174	16:33:04	157	16:40:50	164
16:16:22	156	16:36:17	154	16:44:10	158
16:19:40	152	<b>Total</b>	<b>2630</b>	16:47:30	155
16:22:58	131			16:50:50	162
16:26:21	151			16:54:10	131
16:29:36	163			16:57:30	150
16:32:58	158			17:00:50	138
16:36:24	169			17:04:10	138
16:39:36	151			17:07:30	168
16:42:58	171			17:10:50	172
16:46:27	163			17:14:10	182
16:49:38	132			17:17:30	190
16:52:58	144			17:20:50	153
16:56:18	172			17:24:10	168
16:59:39	130			17:27:30	163
17:02:58	136			17:30:50	174
17:06:16	172			17:34:10	151
17:09:38	162			17:37:30	157
17:13:00	159			17:40:50	107
17:16:19	169			17:44:10	177
17:19:40	168			<b>Total</b>	<b>5531</b>
<b>Total</b>	<b>5603</b>				

**Downstream Volume Counts at the Indian River Road Corridor**

<u>9/21/2021</u>		<u>9/22/2021</u>		<u>9/28/2021</u>	
Time flow ended	Count	Time flow ended	Count	Time flow started	Count
15:10:39	106	15:54:38		16:34:37	171
15:14:09	125	15:57:58	146	16:37:57	150
15:17:19	155	16:01:18	139	16:41:17	156
15:20:47	141	16:04:38	148	16:44:37	157
15:23:39	172	16:07:58	145	<b>Total</b>	<b>634</b>
15:27:19	152	16:11:18	166		
15:30:59	140	<b>Total</b>	<b>744</b>	<b>Time flow started</b>	<b>Count</b>
15:34:09	144			17:14:37	167
15:37:09	149			17:17:57	167
15:40:49	158			17:21:17	179
15:43:59	164			<b>Total</b>	<b>513</b>
15:47:19	162				
15:50:39	142				
15:54:09	155				
15:57:34	159				
16:00:49	150				
16:04:09	139				
16:07:29	149				
16:10:49	164				
16:14:14	159				
16:17:29	145				
16:20:59	137				
16:24:09	153				
16:27:55	156				
16:30:49	143				
16:34:29	173				
16:37:29	133				
16:40:49	175				
16:44:29	157				
16:47:29	128				
16:50:49	136				
16:54:29	162				
16:57:49	135				
17:00:49	135				
17:04:09	166				
17:06:49	150				
<b>Total</b>	<b>5369</b>				